Université de Montréal

Development of Nanostructured Hydrogel for Spatial and Temporal Controlled Release of Active Compounds

By
SHAKER THABIT ALSHARIF

Faculty of Pharmacy

Thesis presented in the Faculty of Pharmacy
to obtain Master degree
in Pharmaceutical Science
option Pharmaceutical Technology

February, 2016

Résumé

L'utilisation de nanovecteurs pour la livraison contrôlée de principes actifs est un concept commun de nous jours. Les systèmes de livraison actuels présentent encore cependant des limites au niveau du taux de relargage des principes actifs ainsi que de la stabilité des transporteurs. Les systèmes composés à la fois de nanovecteurs (liposomes, microgels et nanogels) et d'hydrogels peuvent cependant permettre de résoudre ces problèmes. Dans cette étude, nous avons développé un système de livraison contrôlé se basant sur l'incorporation d'un nanovecteur dans une matrice hydrogel dans le but de combler les lacunes des systèmes se basant sur un vecteur uniquement. Une telle combinaison pourrait permettre un contrôle accru du relargage par stabilisation réciproque. Plus spécifiquement, nous avons développé un hydrogel structuré intégrant des liposomes, microgels et nanogels séparément chargés en principes actifs modèles potentiellement relargués de manière contrôlé. Ce contrôle a été obtenu par la modification de différents paramètres tels que la température ainsi que la composition et la concentration en nanovecteurs. Nous avons comparé la capacité de chargement et la cinétique de relargage de la sulforhodamine B et de la rhodamine 6G en utilisant des liposomes de DOPC et DPPC à différents ratios, des nanogels de chitosan/acide hyaluronique et des microgels de N-isopropylacrylamide (NIPAM) à différents ratios d'acide méthacrylique, incorporés dans un hydrogel modèle d'acrylamide. Les liposomes présentaient des capacités de chargement modérés avec un relargage prolongé sur plus de dix jours alors que les nanogels présentaient des capacités de chargement plus élevées mais une cinétique de relargage plus rapide avec un épuisement de la cargaison en deux jours. Comparativement, les microgels relarguaient complétement leur contenu en un jour. Malgré une cinétique de relargage plus rapide, les microgels ont démontré la possibilité de contrôler finement le chargement en principe actif. Ce contrôle peut être atteint par la modification des propriétés structurelles ou en changeant le milieu d'incubation, comme l'a montré la corrélation avec les isothermes de Langmuir. Chaque système développé a démontré un potentiel contrôle du taux de relargage, ce qui en fait des candidats pour des investigations futures.

Mots-clés : Livraison contrôlée, hydrogel, liposome, microgel, nanogel.

Abstract

Controlled delivery of active compounds using nanoscale carriers is nowadays a common concept, but there are still limitations in current delivery systems related to active compound release rate and nanocarriers stability. To address these limitations, delivery systems can be made to incorporate both nanocarriers (liposomes, microgels and nanogels) and hydrogels. In this study, we have developed controlled delivery systems by combining different carriers in order to overcome deficiencies observed in systems using only one type of carrier. Such a combination could lead to an enhanced controlled release delivery system through synergistic stabilization. More specifically, we created a structured hydrogel embedded with either liposomes, microgels, or nanogels, each loaded with model active compounds that would be released in a controlled fashion by manipulating the temperature of release medium and nanocarriers composition and concentration. We compared drug loading and release kinetics of sulforhodamine B from liposomes (composed of DOPC and DPPC at different ratios) and nanogels (chitosan/hyaluronic acid) embedded in acrylamide hydrogels. We also compared drug loading and release kinetics of rhodamine 6G from microgels of N-isopropylacrylamide (NIPAM) with different ratios of methacrylic acid embedded in acrylamide hydrogel. Liposomes demonstrated a moderate drug loading capacity with sustained release for over ten days, while nanogels showed high drug loading but faster release kinetics, exhausting their contents within two days. Comparatively, microgels completely released their content within a day. Despite their faster release kinetics, microgels have shown the capacity to be finely tuned for efficient drug loading. The Langmuir isotherms indicated that it can be achieved by altering their structural properties or by changing their incubation medium. Each developed system has demonstrated a potential in controlling the release rate, which makes them candidates for further investigations in the future.

Keywords : Controlled delivery, hydrogel, liposome, microgel, nanogel.

Table of contents

List of tables

List of figures

List of abbreviations

AC: Active compound.

AAm: Acrylamide.

BisAc: N, N'-methylene-bis(acrylamide).

CR: Comulative release.

CS: Chitosan.

DL: Drug loading.

DMAEM: N,N′-dimethylamino ethyl methacrylate.

DMPC: Dimyristoyl phosphatidylcholine.

DOPC: Dioleoyl phosphatidylcholine.

DOTAP: 1,2-di-(9-Z-octadecenoyl)-3-trimethyl ammonium propane.

DPPE: Dipalmitoylphosphatidylethanolamine

DPPC: Dipalmitoyl phosphatidylcholine.

ECM: Extra cellular matrix.

ELS: Electrophoretic light scattering.

GlcN: 2-amino-2-deoxy-β-d-glucan.

HA : Hyaluronic acid.

HEPES: N-(2-hydroxyethyl) piperazine-N'-ethanesulfonic acid.

LCST: Lower critical solubility temperature.

LE: Loading efficiency.

LUV: Large unilamellar vesicles.

MAA: Methacrylic acid.

MMA: Methyl methacrylate.

MLV: Multilamellar vesicles.

NIPAM: N-isopropylacrylamide.

PAA: Poly(acrylic acid).

PCL: Polycaprolactone.

PDEA: Poly(N,N-diethylacrylamide).

PdI: Polydispersity indexe.

PDMAEM: Poly(N,N′-diethylamino ethyl methacrylate).

PEG: Polyethylene glycol.

PLA: Polylactic acid.

PLGA: Polylactic-co-glycolic acid. PMA: Poly(methyl acrylate).

PS: Particle size

PPO: Poly(propylene oxide). SDS: Sodium dodecyl sulfate. SUV: Small unilamellar vesicles.

TPP: Sodium tripolyphosphate. UV: Ultraviolet.

ZP: Zeta potential.

2D: Two dimensions.

3D: Three dimensions.

To my parents Thabit Alsharif and Fatimah Alsharif who devoted their lives for me. To my soulmate my wife Randa Alsharif who has been always supportive in my hard times. Last but not least, to my inspiring person during my studies Dr. Xavier Banquy.

Acknowledgement

This project consumed huge amount of work, research, and dedication. Still, implementation would not have been possible if I did not have a support of many individuals. Therefore, I would like to extend my sincere gratitude to all of them.

First of all, I am thankful to Saudi Arabian Cultural Bureau, Royal Embassy of Saudi Arabia for their financial, logistical support, and for providing necessary guidance concerning projects implementation.

I am grateful to Prof. Suzanne Giasson and Prof. Gregoire Leclair for accepting evaluating my thesis. I express my gratitude toward my coleagues in the Faculty of Pharmacy, especially Mohammad Mokhtar, Sarra Zaraa, Pierre-Luc Latreille, Warren Viricel, Jimmy Faivre, Nicolas Hanauer for their kind cooperation and encouragment that helped me for this project completion.

Chapter 1 : Introduction

1.1. Introduction

Active compound (AC) delivery research is one of the most rapidly developing, interdisciplinary fields in science. It is a collaboration between biomedical scientists and health practitioners in order to improve human health care. Advances in active compound delivery systems has led to further improvements in pharmacological activity of different AC dosage forms that had previously limited pharmacokinetic and biodistribution properties. Employment of AC carriers like liposomes, polymeric nanoparticles, and hydrogels has proven to be of importance in developing a controlled delivery system (2-4). Therefore, one of the main approaches is to design a system capable of improving AC efficacy at target tissues, while minimizing its toxicity at healthy tissues (5). A delivery system should be optimized for AC efficacy since it will affect the AC's pharmacokinetic properties, target of action, and side effects.

Hydrogels and liposomes were found to be effective carriers for controlled delivery of multiple active compounds. For instance, anticancer agents (6-8), genetic materials (9-11), and interestingly, growth factors (12-14) that can play a major role in tissue engineering. However, studies found that there are some issues associated with using conventional liposomes alone, including short circulation half-life ($t_{1/2}$) due to rapid uptake by the reticuloendothelial system (15), difficulty in controlling loading and release rate of AC (16-18). Similarly, hydrogels have shown many advantages in different fields, especially in tissue engineering and regenerative medicine but rapid burst release of ACs is a common problem associated with hydrogels as a single delivery system (19-22). Combining AC nanocarriers and hydrogel in a single delivery system could have the potential to create a better controlled delivery, while also addressing concerns about the deficiencies of the individual AC carriers.

1.2. Hydrogels as effective carriers for AC controlled delivery system

Hydrogels have taken on several different definitions since their discovery in 1960 by Wichterle and Limwere (23). The most commonly used definition describes hydrogels as two- or several components system composed of polymeric chain networks containing water that fills hydrogel gaps while remaining insoluble in aqueous media (24). Classification of hydrogel is based on several factors like polymeric composition (mono-polymer or co-polymer) (25), cross-linking method (physically or chemically cross-linked) (26-30), reactivity towards external and physiological stimuli (temperature, pH, magnetic field) (31, 32), and source (natural or synthetic polymers) (33, 34). Moreover, developments in hydrogel technology has lead to increasing its use in the pharmaceutical industry (35).

Hydrogels fabricated from naturally-sourced polymers have multiple advantages making them suitable for pharmaceutical and biomedical applications. Natural polymeric hydrogels usually have better biocompatibility and biodegradability compared to synthetic polymers (36). However, some of these hydrogels do not offer appropriate mechanical features for carrying ACs. Also, they could alter the immune system and cause an inflammatory reaction from pathogens inadvertently embedded in the polymer moieties (37). Alternatively, synthetic hydrogels have polymeric structures that are modifiable to produce the desired mechanical features and degradation kinetics (38-40).

1.3. Hydrogels technologies for improving AC controlled delivery system

Hydrogels for AC controlled delivery goal should have well-defined biodegradability and biocompatibility properties. As a result, there is an increased urge for developing novel and optimized delivery methods. So far, several approaches have been developed to create such hydrogels by manipulating particular parameters, as will be discussed in this section.

1.3.1. Biomimetic hydrogels

Recently, it has been suggested that hydrogel scaffolds as an extra-cellular matrix that mimic normal tissues could improve AC delivery (41-43). As a result, several different fabrication methods have been developed to synthesize such scaffolds (20, 44, 45). Initially, two-dimensional (2D) polymeric scaffolds were used along with adhesive AC for controlled delivery (46, 47). A method was developed based on creating a molecular concentration gradient in the ECM embedding ACs like proteins, macromolecules as chemokines and growth factors (48). Gradient materials were shown to enhance different cellular actions such as cellular proliferation**,** *ex vivo* migration, and transmission of signals (49, 50). For example, a microfluidic gradient instrument composed of poly(ethylene glycol) diacrylate hydrogels was created and placed with MC3T3-E1 cells to generate concentration gradient of okadaic acid as an AC model released by diffusion (51).

Following that**,** three-dimensional (3D) hydrogel scaffolds were developed for improving AC controlled delivery and release through simulating 3D tissues structure. Hydrogels as 3D scaffolds have become very effective in enhancing cell growth, differentiation and organization (52, 53). Several methodologies were developed for embedding AC or cells within hydrogel scaffolds. For instance, one of the primary methods uses cells were embedded within the hydrogel by introducing them during gelation process. An experiment was carried out using human corneal epithelial cells to determine their capacity to survive within calcium alginate-hydroxyethyl cellulose hydrogel. Results showed that insertion of the cells during gelation process did not affect cells activity and survived for seven days at different temperatures. These results revealed that hydrogel can be beneficial to cellular mobilization and storage purposes (54).

A second study discussed the same technique but examined the impact of manipulating hydrogel components over embedded neural stem cells. They incorporated fluorinated methacrylamide chitosan hydrogels containing scaffold elements as ECM to test cells differentiation. According to the study, it had been suggested that Fluorine components in the

hydrogel had a significant role in adjusting oxygen level within the medium, which, significantly enhanced the differentiation of embedded cells (55).

Moreover**,** a new technique making use of niches within alginate hydrogel before embedding hepatocarcinoma cells (HepG2) (56). Gelatin beads of various known diameters were used to create the niches. After that, cells were implanted inside these scaffold cavities and had apparently improved cell proliferation in comparison to scaffolds with no porosity due to superior mass transfer of nutrients and oxygen into the hydrogel.

The lifespan of cells in human tissues are largely influenced by the physical stress, biochemical and physiological properties of the surrounding ECM. Therefore, controlling spatiotemporal factors of ACs and their interaction with cells within tissues are the key to initiate biochemical reactions between them. Using hydrogels as an effective carrier for tissue engineering can provide a combination of cellular encapsulation and triggered release of active compounds to enhance temporally controlled cell growth. For example, a hierarchical porous structure of chitosan hydrogel demonstrating consistent network of pores was developed (57). The hydrogel was prepared by gas foaming after encapsulating $CaCO_3$ microparticles of 10 μm diameter. Then, the hydrogels were freeze-dried to obtain the hierarchical porous structure where molecules of differing charges of chondroitin and chitosan were placed in alternating order to obtain an ECM. In addition, fibroblast growth factors as well as pulmonary fibroblast cells of human origin were loaded into the pores by chondroitin sulfate binding. The results suggested that the network structural design did not negatively impact cumulative release of fibroblast growth factors, and succeeded in supporting cell proliferation by enhancing their loading and promoted their delivery to pulmonary fibroblast cells (57).

Hydrogel scaffolds were tested in injured mice skeletal muscle tissue *in vivo*. The experiment started with mixing alginate hydrogel materials with vascular endothelial growth factor and insulin-like growth factor before gelation procedure takes place as loading method. Next, the mixture was freeze-dried to design niches in the scaffolds in order to embed myoblast cells and to test the scaffold capability for improving muscular tissue regeneration. The authors expressed that vascular endothelial growth factor and insulin-like growth factor

have provided a significant synergistic effect in regenerating damaged tissues. Also, upon loading myoblast cells within the hydrogel, niche scaffolds were more effective for fiber regrowth and improved vascular tissues density, which lead to better healing (58).

In contrast to the above-mentioned methods, a different technique, with implications in orthopedic medicine, based on passive release was developed to facilitate AC interaction with adjacent cells release. They created polyethylene glycol (PEG*)* scaffolds embedding dexamethasone via peptide linker to release AC locally into sites where adjacent human mesenchymal stem cells located. Following that, metalloproteinase were released from stem cells, which breaks down the peptide linkers and suppresses cellular reactions in the hydrogel (59).

1.3.2. Biodegradable hydrogels

Biodegradable hydrogels are preferred over non-degradable hydrogels as carriers within designed conditions because they allow one to control their degradation rate. Consequently, biodegradable hydrogels eliminate the need for surgical extraction after implant procedures (60). However, certain factors and methods during hydrogel fabrication are required to anticipate the degradation levels such as the type of polymer or employing more than one type of polymers with different properties. These factors and techniques are essential in order to achieve optimal controlled release of ACs in implants and tissue regeneration. Hydrolytically degradable hydrogels of PLA-b -PEG-b –poly(lactic acid) (61) have been created using block copolymers of PLA and PEG for protein delivery purposes (62). The degradation rates were investigated in order to determine AC release and diffusion by focusing on certain macroscopic parameters like compressive strength and swelling ratio (63-65). Also, biological moieties have been incorporated into synthetic hydrogels, which allows them to be broken down by enzymes. Peptide substrates were used not only to fabricate biodegradable hydrogel, but also to tailor the rate of degradation and release of ACs (66). For example, in a system created to simulate ECM and its surrounding cells, binding sites were created using integrin and peptide substrates for breakdown by matrix metalloprotease. After that, cells penetrate the hydrogel matrices by matrix metalloproteinase excretion (67, 68).

Another method was developed using a synthetic protein with a degradable matrix to enhance embedding of cells within the hydrogel. The protein has two receptors (RGD integrin and heparin) for cells to attach and two plasmin sites designed to degrade the medium to enhance cell diffusion. The protein has been used in parallel with poly(ethylene glycol) diacrylate to synthesize the hydrogel as ECM encapsulating human fibroblasts-fibrin clusters. Results showed that cell proliferation had been achieved for about seven days while promoting cellular diffusion within the hydrogel (69).

1.3.3. Smart "stimuli-responsive" hydrogels

Stimuli-responsive hydrogels differ from other types of hydrogels in term of their sensitivity to the external parameters like temperature and pH, that affect the rate of swelling of these hydrogels (70). As such, changes in the volume capacity makes this type of hydrogels effective as a controlled delivery system, as the release rate of ACs is adjustable by manipulating external physical parameters (71-73). pH sensitive hydrogels based on pH-sensitive polymers are commonly known as polyelectrolytes. Mostly, polymers used for this purpose include poly(acrylic acid) (PAA) and poly(N,N′-diethylamino ethyl methacrylate) (PDMAEM), which are sensitive to low and high pH respectively (61, 74, 75). As a result, they show different swelling behaviors when fabricated in different pH media. However, employing neutral co-monomers like 2-hydroxyethyl methacrylate, methyl methacrylate and maleic anhydride in pH-sensitive hydrogels can modify and control their pH sensitivity, rate of swelling, and consequently AC release rate (76-78).

Polyelectrolyte hydrogels are widely used for controlling AC release in oral dosage forms because of pH variability along the gastrointestinal tract (77), (79). The method involves embedding caffeine in a hydrogel using copolymers of N,N′-dimethylamino ethyl methacrylate (DMAEM) and methyl methacrylate (MMA). The release of caffeine from hydrogel is only triggered at acidic pH but not at neutral or basic media due to DMAEM sensitivity and ionization at low pH (79).

Thermo-sensitive hydrogels are fabricated from different polymeric materials like poly(N-isopropylacrylamide) (pNIPAM) and Poly(N,N-diethylacrylamide) (PDEA) (80-82). PDEA has been found to be more beneficial due to its lower critical solution temperature LCST, which is relatively close to physiological temperature (83, 84). Unlike the majority of polymers, the water solubility of LCST polymers decrease with increasing temperature which results in hydrogel shrinking (85). The inverse relationship between changes in temperature and swelling rate are due to polymer chains that have either hydrophobic groups or combination of hydrophilic and hydrophobic segments. Hydrogen bonds between aqueous solution molecules and hydrophilic segments are strengthened once the temperature decreased and thus increases polymers dissolution. On the other hand, at higher temperature the hydrogen bonds dissociate and hydrophobic interactions between hydrophobic segments dominate, leading hydrogel shrinking (71).

In order to achieve better control over the swelling and shrinking rate of LCST hydrogels, a technique was developed that modifies hydrophilic and hydrophobic segments ratios by creating copolymers using NIPAM composed of acrylic acid as hydrophobic and hydrophilic monomers respectively (86-88). Applying such method will alter LCST and lead to hydrogels with improved features like responsiveness toward other stimuli and increased shrinking rate upon rising temperature (89). Furthermore, additional types of block copolymers composed of poly(ethylene oxide) (PEO) and poly(propylene oxide) (PPO) share the same features as PDEA in that they have a lower critical solution temperature which can be used to deliver ACs over controlled period of time. Pluronics® (or Poloxamers) is an example of applicable in-situ thermo-sensitive hydrogel using PEO–PPO block copolymers (72, 90).

There are some limitations associated with temperature-sensitive hydrogels using NIPAM for biomedical applications because of issues related to its biodegradability and its metabolism (72). Also, there is a concern related to hydrogels based on acrylamide due to acrylamide's ability to activate platelets once it is in blood stream (91).

1.4. Nanocarriers for AC controlled delivery system

Significant advances in nanotechnology has led to the development of nanoscale carriers with specific physical and chemical properties beneficial for therapeutic purposes (92). Nanocarriers involved in therapeutic applications have been found advantageous in improving controlled delivery of ACs (93). Also, they enhance AC bioavailabity by altering its pharmacokinetic properties and its biodistribution. They may be used as reservoirs for prolonged release in vivo, that is, increasing circulation half-life, and decreasing toxicity of ACs (table 1.1) (94).

Several nanoparticles (NPs) such as polymeric NPs, lipid based NPs (liposomes or micelles), polymer-active compound conjugates, and dendrimers have therapeutic applications (95-97). Nevertheless, choosing the appropriate nanocarier for a specific AC depends on the characteristics of the AC itself, like its potency, shelf life, solubility in different mediums, biochemical charge, and molecular weight (98).

Table 1.1. Common issues related to AC using regular dosage forms, and the potential improvement using nanocarriers (9, 99-103)

Common problems related to AC regular dosage forms	Impact of nanocarriers as delivery system
Low solubility of AC. Some dosage forms are hard to develop like hydrophobic AC in hydrophilic media.	Micelles and liposomes encapsulate hydrophobic and hydrophilic AC.
Tissue toxicity of AC, e.g. (tissue necrosis associated with free doxorubicin).	Controlled release from NPs decreases or eliminates tissue toxicity.
Unwanted pharmacokinetics of AC. Some AC dosage forms experience rapid kidney elimination.	Rapid renal elimination is decreased with small NPs.
Weak biodistribution of AC. Dose limiting side effects associated with expanded AC distribution in some dosage forms.	NPs decrease distribution volume and minimize side effect at non target site
Lack of selectivity of AC in some dosage forms lead to low AC concentration at target site.	NPs enhance selectivity and concentration by ligand-mediated targeting as well as enhanced permeability retention effect respectively

1.4.1. Polymer- active compound conjugates

This type of nanocarrier is used with ACs like proteins and is characterized by having a small molecular weight and non-targeted activity. As a result, this will lead to longer $t_{1/2}$ *in vivo* up to several hours with minimized unwanted side effects through reduction of endocytosis (passive delivery) (104-106). Polysaccharide, polyallylamine hydrochloride, and PEG were the first polymers found to be effective and have been introduced as nanocarriers (107). However, some disadvantages were noticed with these polymers (except PEG. Table 1.2), such as poor biodistribution, short $t_{1/2}$, toxicity, weak AC carrying capability, and fast release (92).

Table 1.2. Different types of PEG-conjugates in clinical use.

PEG-Conjugates	Brand name	Medical indication
PEG-adenosine deaminase	Adagen	Sever combined immunodeficiency with adenosine deaminase deficiency (108).
PEG-anti-VEGF aptamer	Macugen	Macular degeneration (109).
PEG-alfa-interferon 2a	Pegasys	Hep A, Hep C (110).
PEG-GCSF	Neulasta	Neutropnia with cancer chemotherapy (111).
PEG-HGF	Somavert	Acromegally (112).
PEG-L-asparaginase	Oncaspar	Acute lymphoblastic leukemia ALL (113).

1.4.2. Polymer nanoparticles

Polymer nanoparticles production occurs through spontaneous formation of copolymers composed of several polymer blocks with variable hydrophobic ratios (114). Copolymers self-assemble into NPs, exhibiting a hydrophobic core-shell micelles (115). Such nanoparticles are able to carry small amounts of hydrophobic and hydrophilic active compounds. They can also encapsulate macromolecules like protiens (116, 117). The most frequently employed polymers to synthesize nanoparticles are poly D,L-lactic acid, poly D,L-glycolic acid, and poly **Σ-**carpolactone along with copolymers in different ratios surrounded by PEG (118, 119). Many techniques through which the controlled release can be achieved, such as polymers side chain alteration, and copolymer synthesis development (120-123). Abraxane® and Zevalin® are examples of commercially available NPs for medical applications (124).

1.4.3. Liposomes for AC controlled delivery system

After Alec Bangham discovered liposomes 40 years ago, liposomes have become ubiquitous in medical and pharmaceutical research as a fundamental tool in AC controlled delivery systems. Liposomes are lipid-based nanoparticles, 100 – 5000 nm in diameter, composed of a bi-layered vesicle with a hydrophilic core (125). The basic building blocks of liposomes are amphiphilic molecules such as phospholipids. These phospholipids have hydrophilic heads composed of phosphoric acid with a hydrophobic tail consisting of two chains of fatty acids, 10-24 carbon atoms in length, with 0-6 double covalent bonds in every chain (figure 1.1) (126, 127). Liposome formation is initiated through phospholipid hydration in water while applying multiple energy inputs of heating and sonication. Moreover, this process can lead to the formation of lamellar sheets in which hydrophilic heads are facing the aqueous area, while hydrophobic chains are facing each other, forming a-vesicle like structure with a hydrophilic core (128).

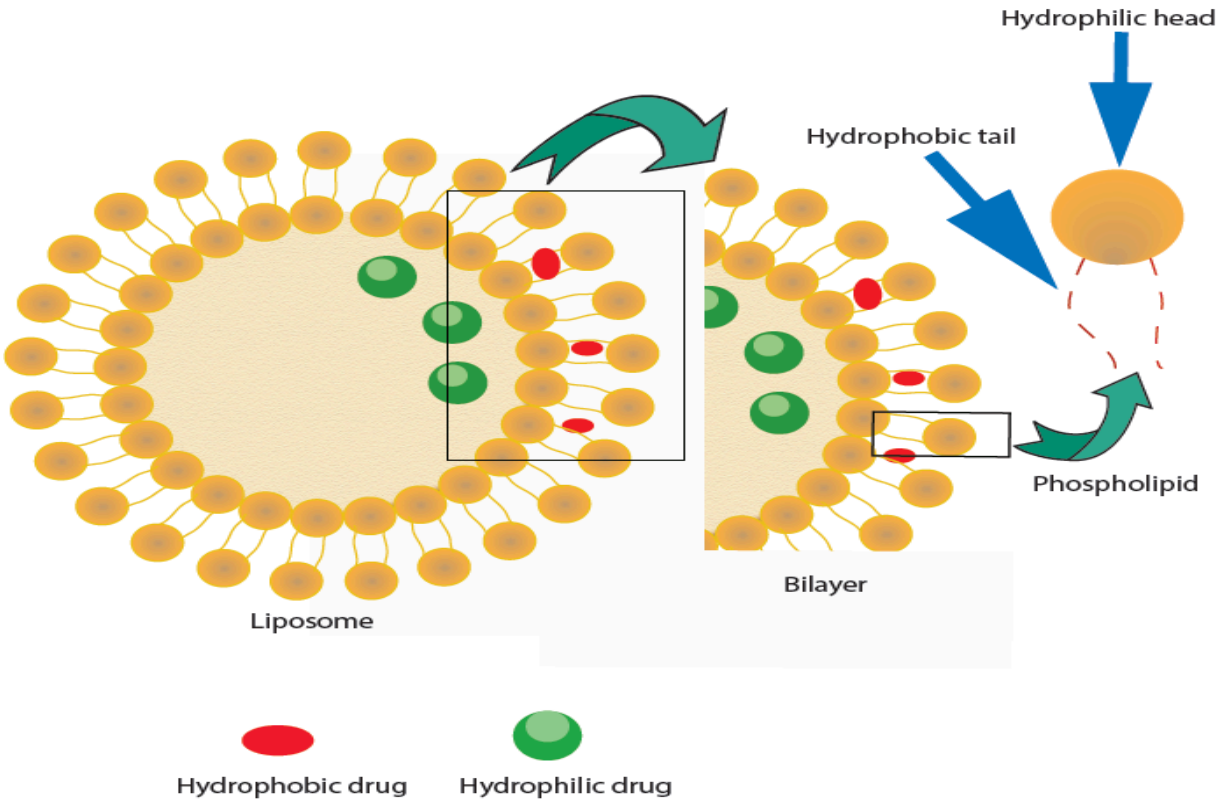

Figure 1.1. Schematic diagram of phospholipids and liposome structure.

Liposomes can be classified according to size, structure, and quantity of bilayers. Nevertheless, the discussion will focus on classification in terms of size and bilayers quantity exclusively into multilamellar vesicle (MLV), large unilamellar vesicle (LUV), and small unilamellar vesicle (SUV) as described in figure 1.2.

Multilamellar vesicles (MLV)

These types of liposomes are greater than 100 nm in size and contain two or more bilayers. MLV are prepared by slow rate thin film hydration method to improve active compound encapsulation and characterized by mechanical stability for extended duration (129). MLV elimination occurs rapidly through reticulo endothelial system (RES) because of its large size (130).

Large unilamellar vesicle (LUV)

Although LUV liposome has a similar size to MLV, it has only a single bilayer. Also, LUV requires only small amount of lipids to encapsulate a larger quantity or volume of hydrophilic AC comparing to MLV (130, 131). Freeze-thawing method is one among several methods to prepare such liposomes formulation (132, 133). Rapid RES elimination is still the predominant issue with this class of liposomes.

Small unilalmellar vesicle (SUV)

Usually, this class of liposomes is defined as having a diameter less than or equal to 100 nm. They have low encapsulation efficiency and prolonged *in vivo* circulation in comparison to other types of liposomes. It is common to use an extrusion process for restricting the size to obtain SUV liposomes (134).

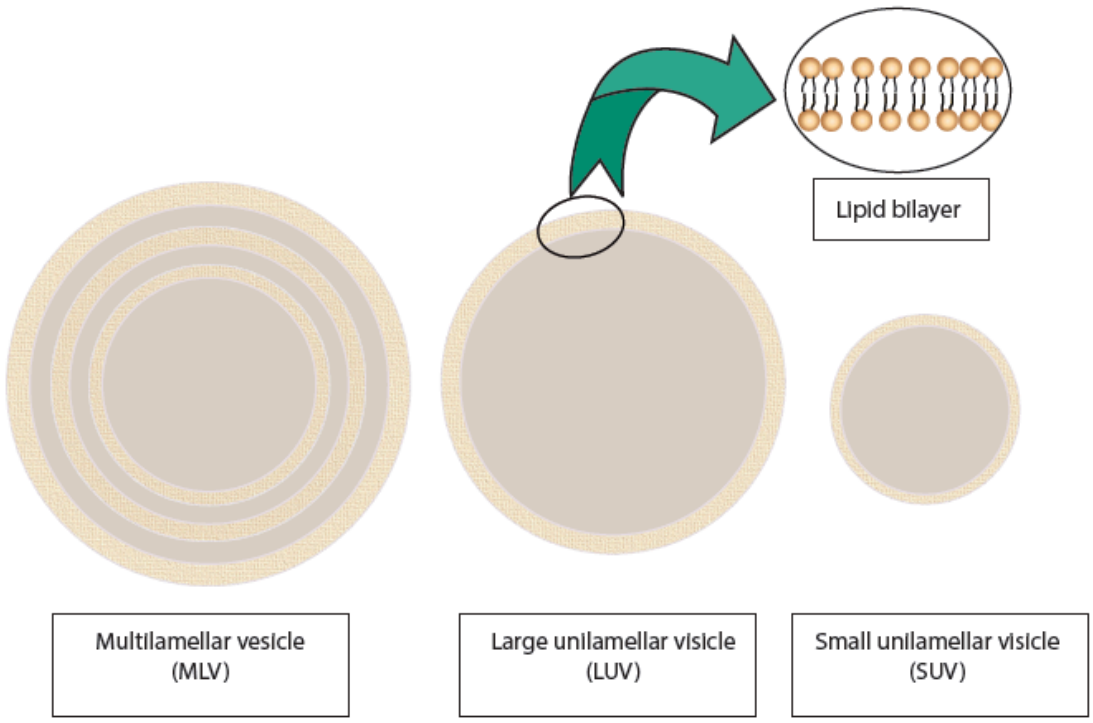

Figure 1.2. Schematic diagram of liposomes classification based on size and bilayers number.

1.4.4. Liposomes technologies for AC controlled delivery system development

In this section, applications and developed technologies to enhance liposomal efficiency will be discussed since liposomes were central to the project.

1.4.4.1. Targeting liposomes for AC controlled delivery system

Many ACs are well known for their systemic or localized toxicity due to their high potency and narrow therapeutic indexes. In order to achieve an optimal delivery to the affected sites without exposing other non-affected sites to further toxicity, formulating liposomes encapsulating active compounds has been suggested for better convenience and efficacy. Active and passive targeting mechanisms for creating targeting liposomes have been proposed

(135-137). For instance, a (passive/active mechanism) involving IgG Immunoglobulins and their segments has been commonly used in order to create targeting moieties in immunoliposomes without impacting their structural integrity. IgG Immunoglobulins attached to liposome surface via covalent bonds or inserted within liposome membrane through hydrophobic interaction (138). Despite developments in liposomal targeting, most liposomes undergo hepatic accumulation and metabolize due to their short $t_{1/2}$ at targeted sites. Enhancing liposomal $t_{1/2}$ would lead to improved interaction and accumulation at target sites instead of liver.

1.4.4.2. Long circulating liposomes for AC controlled delivery system

Several methods were suggested to manage controlled delivery and release rate that lead to prolonged, consistent, and effective therapeutic plasma level of ACs (139-141). They involve liposome surface modifications by altering liposome pH sensitivity, managing particle liposome size, and manipulating liposome-melting temperature by choosing different phospholipids with different transition temperature (table 1.3) (127, 130, 134).

In addition, surface modification of liposomes with biocompatible polymers such as PEG has shown ptential as an effective method in achieving long-circulating liposomes (142, 143). These biocompatible polymers are flexible and facilitate the formation protective impermeable layer around the liposome via surface grafting molecules (144, 145). However, the attachment of PEG polymers on the liposome surface has to be reversible to allow liposomal uptake by cells. Disassembly of PEG from liposome occurs by the effect of pathological factors as the liposome approaches the target cell by enhanced permeability and retention (EPR) (146). Polymers like poly[N-(2-hydroxypropyl) methacrylamide)], poly-N-vinylpyrrolidones, and polyvinyl alcohol were also used for synthesizing long-circulating liposomes (147-149).

Another method to create long-circulating liposomes is by altering liposome pH sensitivity. It can be achieved by creating novel lipid compositions, modifying liposome structure using pH-sensitive polymers, or combining both methods to extend liposomal $t_{1/2}$ and

improve targeting. A pH-sensitive liposome with a PEG-modified surface is an example of long-circulating liposome that has efficient pH sensitivity allowing it to deliver and release ACs inside target cell (139). Also, liposomes composed of a pH-sensitive phospholipids, such as phosphatidylethanolamine (PE), were developed to release antisense oligonucleotides following liposomal degradation at acidic pH only (150). Further pH sensitive components for liposomal manipulation were discovered and discussed (151-153). Long-circulating liposomes have indicated enhanced bioavailability as discovered in several clinical studies (137, 154, 155).

Table 1.3. Examples of phospholipids used in liposome synthesis and their transition temperatures (127, 130, 134).

Phospholipids	**Phase transition ^{O}C**
Dimyristoyl phosphatidylcholine (DMPC)	23
Dioleoyl phosphatidylcholine (DOPC)	-22
Distearoyl phosphatidylcholine (DSPC)	55
Dipalmitoyl phosphatidylethanolamine (DPPE)	67
Dipalmitoyl phosphatidylcholine (DPPC)	41

1.5. Limitations of liposomes and hydrogels as carriers for controlled delivery system

Usually, liposomes are known to be safe and biocompatible, but in some cases like cationic liposomes they show some cytotoxicity specifically when administered in elevated doses (156). Furthermore, liposomes are difficult to sterilize since chemical agents may cause liposomal instability. Thus far, a filtration process using 220 nm membranes is the only recommended sterilizing method (130). Short shelf life and stability of liposomes are major concerns because of the difficulty with keeping liposomes stored for periods similar to other dosage forms. Liposomal stability is significantly influenced by chemical (oxidation or hydrolysis) and physical (aggregation or temperature) factors (157-159). Moreover, liposomes express very low encapsulation efficiency, which could affect the therapeutic efficacy if loaded AC does not meet required doses to be delivered. Although some studies discussed increasing liposomal encapsulation efficiency, hydrophobic ACs encapsulation remains less efficient compared to hydrophilic ACs (160-162).

Hydrogels as AC carriers have shown variable biocompatibility rates based on their polymeric monomers and cross-linkers compositions (163). Several disadvantages exist, such as reduced mechanical strength, where AC loading becomes less eficient (164). Also, rapid burst release of ACs from hydrogel matrices due to their high water content and moderately large network pores is a common issue (165). Similarly to liposomes, the sterilization process of hydrogels remains a challenge (34).

The above-mentioned drawbacks to liposomes and hydrogels as separate carriers are limiting their potentials to provide optimal controlled delivery of ACs, thus increasing the need to develop novel methods allowing these carriers to be improved for biomedical and pharmaceutical applications. Developing a system based on combining hydrogel with nanocarrier such as liposome could overcome some of the limitations associated with each system separately, especially those affecting the release rate. For instance, stability concern related to liposomes that lead to rapid release of ACs can be improved via embedding them into hydrogel (see below, 1.6).

1.6. Synergistic combination of nanocarriers with hydrogel as a novel controlled delivery system

Synergistic combination of different carriers as a novel controlled delivery system has attracted attention because of the capability for administrating several ACs while also controlling their release rate. Consequently, minimized side effects and improved therapeutic profiles can be achieved with lower dosage requirements (166-168). Systems that combine hydrogels cross-linking with either polymers or lipid based nanoparticles have been discussed in previous studies (169-171). For example, manipulating certain parameters icluding hydrogel polymer properties, concentration and composition of liposomes, as well as their interaction with hydrogels (e.g., swelling rate) can alter liposomes stuctural integrity and improve mechanical stability (172, 173).

The loading process of any bioactive molecule either hormonal or synthetic therapeutic agents into hydrogel scaffolds, is accomplished through employing different chemical and physical binding factors (covalent bonding or electrostatic interaction) (174). In order to achieve improved spatial and temporal controlled release and delivery of ACs, manipulation of chemical and physical bindings within hydrogels is required (175). Still, the major concern about embedding bioactive compounds into hydrogels is the initial burst release or complete fast release of ACs. It is difficult to perfectly manage hydrogel network design completely with the developed synthetic methods so far, which in turn affects ACs release rate and efficacy (176, 177). To find a solutions to manage the burst effect and to improve ACs loading in hydrogel, two different nanoparticles of N-(2-hydroxyl) propyl-3-trimethyl ammonium chitosan chloride and carboxymethyl chitosan were mixed and embedded within a chitosan/poly(vinyl alcohol) hydrogel before gelation process. Propranolol (positively charged) and diclofenac sodium (negatively charged) were used as ACs. Controlling the release rate of ACs was obtained through altering the nanoparticles ratio embedded within the hydrogel (178).

To enhance AC controlled delivery, a recently developed technique uses two AC carriers of liposomes and hydrogels for topical administration (179). Cationic pH sensitive liposomes composed of L-phosphatidylcholine (PC) and 1,2-di-(9-Z-octadecenoyl)-3-trimethyl ammonium propane (DOTAP) phospholipids were prepared and stabilized using gold nanoparticles. Then, the stabilized liposomes loaded with rhodamine B were embedded into polyacrylamide hydrogels at various cross-linking rates to investigate viscoelasticity effects over release kinetics. Results indicated that modifying cross-linking rate and the pH of the medium has a major effect not only on AC release, but also over the release of stabilized liposomes from hydrogel matrices (179).

1.7. Hypothesis and objectives

Previously, hydrogels have been used as active compound delivery systems, but in some cases hydrogels suffer from rapid burst release of loaded active compounds. However, incorporating a secondary system such as liposomes could overcome the limitations of hydrogels in a synergistic manner since it could improve the stability of active compounds and their controlled release. Therefore, the main objective is to combine two active compound delivery systems in order to counteract deficiencies observed in the individual systems such that it would lead to an enhanced controlled release delivery system. More specifically, the goal is to develop a structured hydrogel with embedded liposomes loaded with active compounds that would be released in a controlled fashion.

The first objective is to prepare and characterize three liposomal formulations using different concentrations of different components of phospholipids loaded with sulforhodamine B as the active compound. Following that, the effects of varying phospholipids ratios and thermal conditions on active compound release rate will be evaluated.

The second objective is to synthesize and optimize hydrogels with a fixed cross-linking degree by a photopolymerization process using an acrylamide monomer, N, N'-methylene-bis(acrylamide) cross-linker, and Irgacure® photoinitiator. Furthermore, three different controlled delivery systems based on three different liposomal formulations, each with a different phospholipid composition, embedded in a hydrogel loaded with sulforhodamine B prior to the gelation process will be developed. This will serve as a basis for studying the release rate of model active compound under different thermal conditions. Comparing results from both liposomes alone and liposomes embedded in hydrogels would indicate whether a combined system is capable of providing an extended release rate of active compounds.

1.8. References

1. Laouini A, Jaafar-Maalej C, Limayem-Blouza I, Sfar S, Charcosset C, Fessi H. Preparation, Characterization and Applications of Liposomes: State of the Art. Journal of Colloid Science and Biotechnology. 2012;1(2):147-68.

2. Hughes GA. Nanostructure-mediated drug delivery. Nanomedicine: nanotechnology, biology and medicine. 2005;1(1):22-30.

3. Rawat M, Singh D, Saraf S, Saraf S. Nanocarriers: promising vehicle for bioactive drugs. Biological and Pharmaceutical Bulletin. 2006;29(9):1790-8.

4. Peer D, Karp JM, Hong S, Farokhzad OC, Margalit R, Langer R. Nanocarriers as an emerging platform for cancer therapy. Nature nanotechnology. 2007;2(12):751-60.

5. Xiang T-X, Anderson BD. Liposomal drug transport: a molecular perspective from molecular dynamics simulations in lipid bilayers. Advanced drug delivery reviews. 2006;58(12):1357-78.

6. Hofheinz R-D, Gnad-Vogt SU, Beyer U, Hochhaus A. Liposomal encapsulated anti-cancer drugs. Anti-cancer drugs. 2005;16(7):691-707.

7. Ta HT, Dass CR, Dunstan DE. Injectable chitosan hydrogels for localised cancer therapy. Journal of Controlled Release. 2008;126(3):205-16.

8. Mao L, Wang H, Tan M, Ou L, Kong D, Yang Z. Conjugation of two complementary anti-cancer drugs confers molecular hydrogels as a co-delivery system. Chemical Communications. 2012;48(3):395-7.

9. Gregoriadis G. Liposome technology. Volume II: Incorporation of drugs, proteins and genetic material. 1984.

10. Gao X, Huang L. Potentiation of cationic liposome-mediated gene delivery by polycations. Biochemistry. 1996;35(3):1027-36.

11. Krebs MD, Jeon O, Alsberg E. Localized and sustained delivery of silencing RNA from macroscopic biopolymer hydrogels. Journal of the American chemical Society. 2009;131(26):9204-6.

12. Yamamoto M, Ikada Y, Tabata Y. Controlled release of growth factors based on biodegradation of gelatin hydrogel. Journal of Biomaterials Science, Polymer Edition. 2001;12(1):77-88.

13. Lee KY, Peters MC, Anderson KW, Mooney DJ. Controlled growth factor release from synthetic extracellular matrices. Nature. 2000;408(6815):998-1000.
14. Willis MC, Collins B, Zhang T, Green LS, Sebesta DP, Bell C, et al. Liposome-Anchored Vascular Endothelial Growth Factor Aptamers §. Bioconjugate chemistry. 1998;9(5):573-82.
15. Allen TM, Hansen C, Rutledge J. Liposomes with prolonged circulation times: factors affecting uptake by reticuloendothelial and other tissues. Biochimica et Biophysica Acta (BBA)-Biomembranes. 1989;981(1):27-35.
16. Kulkarni S, Betageri G, Singh M. Factors affecting microencapsulation of drugs in liposomes. Journal of microencapsulation. 1995;12(3):229-46.
17. Lasic DD. Novel applications of liposomes. Trends in biotechnology. 1998;16(7):307-21.
18. Charrois GJ, Allen TM. Drug release rate influences the pharmacokinetics, biodistribution, therapeutic activity, and toxicity of pegylated liposomal doxorubicin formulations in murine breast cancer. Biochimica et Biophysica Acta (BBA)-Biomembranes. 2004;1663(1):167-77.
19. Drury JL, Mooney DJ. Hydrogels for tissue engineering: scaffold design variables and applications. Biomaterials. 2003;24(24):4337-51.
20. Nguyen KT, West JL. Photopolymerizable hydrogels for tissue engineering applications. Biomaterials. 2002;23(22):4307-14.
21. Lin C-C, Anseth KS. PEG hydrogels for the controlled release of biomolecules in regenerative medicine. Pharmaceutical research. 2009;26(3):631-43.
22. Sershen S, Westcott S, Halas N, West J. Temperature‐sensitive polymer–nanoshell composites for photothermally modulated drug delivery. Journal of biomedical materials research. 2000;51(3):293-8.
23. Kopecek J. Hydrogels: From soft contact lenses and implants to self‐assembled nanomaterials. Journal of Polymer Science Part A: Polymer Chemistry. 2009;47(22):5929-46.
24. Ahmed EM. Hydrogel: preparation, characterization, and applications. Journal of advanced research. 2013.
25. Iizawa T, Taketa H, Maruta M, Ishido T, Gotoh T, Sakohara S. Synthesis of porous poly (N‐isopropylacrylamide) gel beads by sedimentation polymerization and their morphology. Journal of applied polymer science. 2007;104(2):842-50.

26. Hoare TR, Kohane DS. Hydrogels in drug delivery: progress and challenges. Polymer. 2008;49(8):1993-2007.
27. Chen PC, Kohane DS, Park YJ, Bartlett RH, Langer R, Yang VC. Injectable microparticle–gel system for prolonged and localized lidocaine release. II. In vivo anesthetic effects. Journal of Biomedical Materials Research Part A. 2004;70(3):459-66.
28. Chen PC, Park YJ, Chang LC, Kohane DS, Bartlett RH, Langer R, et al. Injectable microparticle-gel system for prolonged and localized lidocaine release. I. In vitro characterization. Journal of Biomedical Materials Research Part A. 2004;70(3):412-9.
29. Kurisawa M, Chung JE, Yang YY, Gao SJ, Uyama H. Injectable biodegradable hydrogels composed of hyaluronic acid–tyramine conjugates for drug delivery and tissue engineering. Chemical communications. 2005(34):4312-4.
30. Jin R, Hiemstra C, Zhong Z, Feijen J. Enzyme-mediated fast in situ formation of hydrogels from dextran–tyramine conjugates. Biomaterials. 2007;28(18):2791-800.
31. Park TG. Temperature modulated protein release from pH/temperature-sensitive hydrogels. Biomaterials. 1999;20(6):517-21.
32. Brazel CS. Magnetothermally-responsive nanomaterials: combining magnetic nanostructures and thermally-sensitive polymers for triggered drug release. Pharmaceutical research. 2009;26(3):644-56.
33. Zhao W, Jin X, Cong Y, Liu Y, Fu J. Degradable natural polymer hydrogels for articular cartilage tissue engineering. Journal of Chemical Technology and Biotechnology. 2013;88(3):327-39.
34. Hoffman AS. Hydrogels for biomedical applications. Advanced drug delivery reviews. 2012;64:18-23.
35. Kashyap N, Kumar N, Kumar MR. Hydrogels for pharmaceutical and biomedical applications. Critical Reviews™ in Therapeutic Drug Carrier Systems. 2005;22(2).
36. Mano J, Silva G, Azevedo HS, Malafaya P, Sousa R, Silva S, et al. Natural origin biodegradable systems in tissue engineering and regenerative medicine: present status and some moving trends. Journal of the Royal Society Interface. 2007;4(17):999-1030.
37. Lin C-C, Metters AT. Hydrogels in controlled release formulations: network design and mathematical modeling. Advanced drug delivery reviews. 2006;58(12):1379-408.

38. Wang C, Stewart RJ, KopeČek J. Hybrid hydrogels assembled from synthetic polymers and coiled-coil protein domains. Nature. 1999;397(6718):417-20.
39. Hong Y, Huber A, Takanari K, Amoroso NJ, Hashizume R, Badylak SF, et al. Mechanical properties and in vivo behavior of a biodegradable synthetic polymer microfiber–extracellular matrix hydrogel biohybrid scaffold. Biomaterials. 2011;32(13):3387-94.
40. Lutolf M, Hubbell J. Synthetic biomaterials as instructive extracellular microenvironments for morphogenesis in tissue engineering. Nature biotechnology. 2005;23(1):47-55.
41. Yang S, Leong K-F, Du Z, Chua C-K. The design of scaffolds for use in tissue engineering. Part I. Traditional factors. Tissue engineering. 2001;7(6):679-89.
42. Yang S, Leong K-F, Du Z, Chua C-K. The design of scaffolds for use in tissue engineering. Part II. Rapid prototyping techniques. Tissue engineering. 2002;8(1):1-11.
43. Rabanel JM, Banquy X, Zouaoui H, Mokhtar M, Hildgen P. Progress technology in microencapsulation methods for cell therapy. Biotechnology progress. 2009;25(4):946-63.
44. Hutmacher D, Goh J, Teoh S. An introduction to biodegradable materials for tissue engineering applications. Annals of the Academy of Medicine, Singapore. 2001;30(2):183-91.
45. Pham QP, Sharma U, Mikos AG. Electrospinning of polymeric nanofibers for tissue engineering applications: a review. Tissue engineering. 2006;12(5):1197-211.
46. Rezwan K, Chen Q, Blaker J, Boccaccini AR. Biodegradable and bioactive porous polymer/inorganic composite scaffolds for bone tissue engineering. Biomaterials. 2006;27(18):3413-31.
47. Nikolovski J, Mooney DJ. Smooth muscle cell adhesion to tissue engineering scaffolds. Biomaterials. 2000;21(20):2025-32.
48. Hanauer N, Latreille PL, Alsharif S, Banquy X. 2D, 3D and 4D Active Compound Delivery in Tissue Engineering and Regenerative Medicine. Current pharmaceutical design. 2015;21(12):1506-16.
49. Singh M, Berkland C, Detamore MS. Strategies and applications for incorporating physical and chemical signal gradients in tissue engineering. Tissue Engineering Part B: Reviews. 2008;14(4):341-66.
50. Sant S, Hancock MJ, Donnelly JP, Iyer D, Khademhosseini A. Biomimetic gradient hydrogels for tissue engineering. The Canadian journal of chemical engineering. 2010;88(6):899-911.

51. Ostrovidov S, Annabi N, Seidi A, Ramalingam M, Dehghani F, Kaji H, et al. Controlled release of drugs from gradient hydrogels for high-throughput analysis of cell–drug interactions. Analytical chemistry. 2012;84(3):1302-9.
52. Lee J, Cuddihy MJ, Kotov NA. Three-dimensional cell culture matrices: state of the art. Tissue Engineering Part B: Reviews. 2008;14(1):61-86.
53. Nicodemus GD, Bryant SJ. Cell encapsulation in biodegradable hydrogels for tissue engineering applications. Tissue Engineering Part B: Reviews. 2008;14(2):149-65.
54. Wright B, Cave RA, Cook JP, Khutoryanskiy VV, Mi S, Chen B, et al. Enhanced viability of corneal epithelial cells for efficient transport/storage using a structurally modified calcium alginate hydrogel. Regenerative medicine. 2012;7(3):295-307.
55. Li H, Wijekoon A, Leipzig ND. Encapsulated neural stem cell neuronal differentiation in fluorinated methacrylamide chitosan hydrogels. Annals of biomedical engineering. 2014;42(7):1456-69.
56. Hwang CM, Sant S, Masaeli M, Kachouie NN, Zamanian B, Lee S-H, et al. Fabrication of three-dimensional porous cell-laden hydrogel for tissue engineering. Biofabrication. 2010;2(3):035003.
57. Du M, Zhu Y, Yuan L, Liang H, Mou C, Li X, et al. Assembled 3D cell niches in chitosan hydrogel network to mimic extracellular matrix. Colloids and Surfaces A: Physicochemical and Engineering Aspects. 2013;434:78-87.
58. Borselli C, Cezar CA, Shvartsman D, Vandenburgh HH, Mooney DJ. The role of multifunctional delivery scaffold in the ability of cultured myoblasts to promote muscle regeneration. Biomaterials. 2011;32(34):8905-14.
59. Yang C, Mariner PD, Nahreini JN, Anseth KS. Cell-mediated delivery of glucocorticoids from thiol-ene hydrogels. Journal of Controlled Release. 2012;162(3):612-8.
60. Park H, Park K, Shalaby WS. Biodegradable hydrogels for drug delivery: CRC Press; 2011.
61. Plamper FA, Ruppel M, Schmalz A, Borisov O, Ballauff M, Müller AH. Tuning the thermoresponsive properties of weak polyelectrolytes: aqueous solutions of star-shaped and linear poly (N, N-dimethylaminoethyl methacrylate). Macromolecules. 2007;40(23):8361-6.
62. West JL, Hubbell JA. Photopolymerized hydrogel materials for drug delivery applications. Reactive Polymers. 1995;25(2):139-47.

63. Metters AT, Bowman CN, Anseth KS. A statistical kinetic model for the bulk degradation of PLA-b-PEG-b-PLA hydrogel networks. The Journal of Physical Chemistry B. 2000;104(30):7043-9.
64. Metters AT, Anseth KS, Bowman CN. A statistical kinetic model for the bulk degradation of PLA-b-PEG-b-PLA hydrogel networks: Incorporating network non-idealities. The Journal of Physical Chemistry B. 2001;105(34):8069-76.
65. Mason MN, Metters AT, Bowman CN, Anseth KS. Predicting controlled-release behavior of degradable PLA-b-PEG-b-PLA hydrogels. Macromolecules. 2001;34(13):4630-5.
66. Hu B-H, Messersmith PB. Rational design of transglutaminase substrate peptides for rapid enzymatic formation of hydrogels. Journal of the American chemical society. 2003;125(47):14298-9.
67. Lutolf M, Lauer-Fields J, Schmoekel H, Metters A, Weber F, Fields G, et al. Synthetic matrix metalloproteinase-sensitive hydrogels for the conduction of tissue regeneration: engineering cell-invasion characteristics. Proceedings of the National Academy of Sciences. 2003;100(9):5413-8.
68. Lutolf MP, Raeber GP, Zisch AH, Tirelli N, Hubbell JA. Cell-Responsive Synthetic Hydrogels. Advanced Materials. 2003;15(11):888-92.
69. Halstenberg S, Panitch A, Rizzi S, Hall H, Hubbell JA. Biologically engineered protein-graft-poly (ethylene glycol) hydrogels: a cell adhesive and plasmin-degradable biosynthetic material for tissue repair. Biomacromolecules. 2002;3(4):710-23.
70. Akala EO, Kopečková P, Kopeček J. Novel pH-sensitive hydrogels with adjustable swelling kinetics. Biomaterials. 1998;19(11):1037-47.
71. Qiu Y, Park K. Environment-sensitive hydrogels for drug delivery. Advanced drug delivery reviews. 2012;64:49-60.
72. Bromberg LE, Ron ES. Temperature-responsive gels and thermogelling polymer matrices for protein and peptide delivery. Advanced drug delivery reviews. 1998;31(3):197-221.
73. Kost J, Langer R. Responsive polymeric delivery systems. Advanced drug delivery reviews. 2012;64:327-41.
74. Huang Y, Yu H, Xiao C. pH-sensitive cationic guar gum/poly (acrylic acid) polyelectrolyte hydrogels: Swelling and in vitro drug release. Carbohydrate Polymers. 2007;69(4):774-83.

75. Wu W, Liu J, Cao S, Tan H, Li J, Xu F, et al. Drug release behaviors of a pH sensitive semi-interpenetrating polymer network hydrogel composed of poly (vinyl alcohol) and star poly [2-(dimethylamino) ethyl methacrylate]. International journal of pharmaceutics. 2011;416(1):104-9.
76. Falamarzian M, Varshosaz J. The effect of structural changes on swelling kinetics of polybasic/hydrophobic pH-sensitive hydrogels. Drug development and industrial pharmacy. 1998;24(7):667-9.
77. Brannon-Peppas L, Peppas NA. Dynamic and equilibrium swelling behaviour of pH-sensitive hydrogels containing 2-hydroxyethyl methacrylate. Biomaterials. 1990;11(9):635-44.
78. Khare AR, Peppas NA. Release behavior of bioactive agents from pH-sensitive hydrogels. Journal of Biomaterials Science, Polymer Edition. 1993;4(3):275-89.
79. Siegel RA, Falamarzian M, Firestone BA, Moxley BC. pH-controlled release from hydrophobic/polyelectrolyte copolymer hydrogels. Journal of controlled release. 1988;8(2):179-82.
80. Zhang J, Chu L-Y, Li Y-K, Lee YM. Dual thermo-and pH-sensitive poly (N-isopropylacrylamide-co-acrylic acid) hydrogels with rapid response behaviors. Polymer. 2007;48(6):1718-28.
81. Vihola H, Laukkanen A, Valtola L, Tenhu H, Hirvonen J. Cytotoxicity of thermosensitive polymers poly (N-isopropylacrylamide), poly (N-vinylcaprolactam) and amphiphilically modified poly (N-vinylcaprolactam). Biomaterials. 2005;26(16):3055-64.
82. Ngadaonye JI, Geever LM, Cloonan MO, Higginbotham CL. Photopolymerised thermo-responsive poly (N, N-diethylacrylamide)-based copolymer hydrogels for potential drug delivery applications. Journal of Polymer Research. 2012;19(3):1-15.
83. Liu H, Zhu X. Lower critical solution temperatures of N-substituted acrylamide copolymers in aqueous solutions. Polymer. 1999;40(25):6985-90.
84. Chen J, Liu M, Liu H, Ma L. Synthesis, swelling and drug release behavior of poly (N, N-diethylacrylamide-co-N-hydroxymethyl acrylamide) hydrogel. Materials Science and Engineering: C. 2009;29(7):2116-23.
85. Shibanuma T, Aoki T, Sanui K, Ogata N, Kikuchi A, Sakurai Y, et al. Thermosensitive Phase-Separation Behavior of Poly (acrylic acid)-g raft-poly (N, N-dimethylacrylamide) Aqueous Solution. Macromolecules. 2000;33(2):444-50.

86. Schild HG. Poly (N-isopropylacrylamide): experiment, theory and application. Progress in polymer science. 1992;17(2):163-249.
87. Feil H, Bae Y, Feijen J, Kim S. Mutual influence of pH and temperature on the swelling of ionizable and thermosensitive hydrogels. Macromolecules. 1992;25(20):5528-30.
88. Hirotsu S. Coexistence of phases and the nature of first-order phase transition in poly-N-isopropylacrylamide gels. Responsive Gels: Volume Transitions II: Springer; 1993. p. 1-26.
89. Dong L-C, Hoffman AS. Synthesis and application of thermally reversible heterogels for drug delivery. Journal of controlled release. 1990;13(1):21-31.
90. Edsman K, Carlfors J, Petersson R. Rheological evaluation of poloxamer as an in situ gel for ophthalmic use. European journal of pharmaceutical sciences. 1998;6(2):105-12.
91. Merril E, Pekala RW. Hydrogel for blood contact. Hydrogels in medicine and pharmacy. 1987;3.
92. Wang AZ, Gu F, Zhang L, Chan JM, Radovic-Moreno A, Shaikh MR, et al. Biofunctionalized targeted nanoparticles for therapeutic applications. 2008.
93. Wagner V, Dullaart A, Bock A-K, Zweck A. The emerging nanomedicine landscape. Nature biotechnology. 2006;24(10):1211-7.
94. Allen TM, Cullis PR. Drug delivery systems: entering the mainstream. Science. 2004;303(5665):1818-22.
95. Liu M, Kono K, Fréchet JM. Water-soluble dendritic unimolecular micelles:: Their potential as drug delivery agents. Journal of Controlled Release. 2000;65(1):121-31.
96. Moghimi SM, Hunter AC, Murray JC. Long-Circulating and Target-Specific Nanoparticles: Theory to Practice. Pharmacological Reviews. 2001;53(2):283-318.
97. Lavan DA, McGuire T, Langer R. Small-scale systems for in vivo drug delivery. Nature biotechnology. 2003;21(10):1184-91.
98. De Jong WH, Borm PJ. Drug delivery and nanoparticles: applications and hazards. International journal of nanomedicine. 2008;3(2):133.
99. Gregoriadis G. Liposomes as drug carriers: recent trends and progress: Wiley Chichester; 1988.
100 . Lasic DD. Liposomes: from physics to applications: Elsevier Science Ltd; 1993.
101. Lasic DD, Martin FJ. Stealth liposomes: CRC press; 1995.

102. Woodle MC, Storm G. Long circulating liposomes: old drugs, new therapeutics: Springer Science & Business Media; 1998.
103. Lasic DD, Papahadjopoulos D. Medical applications of liposomes: Elsevier; 1998.
104. Kaur K, Aggarwal G, Harikumar S. Nanomedicine In Cancer: A Concise Review.
105. Tanaka T, Shiramoto S, Miyashita M, Fujishima Y, Kaneo Y. Tumor targeting based on the effect of enhanced permeability and retention (EPR) and the mechanism of receptor-mediated endocytosis (RME). International journal of pharmaceutics. 2004;277(1):39-61.
106. Deguchi J-o, Aikawa M, Tung C-H, Aikawa E, Kim D-E, Ntziachristos V, et al. Inflammation in Atherosclerosis Visualizing Matrix Metalloproteinase Action in Macrophages In Vivo. Circulation. 2006;114(1):55-62.
107. Davis FF. The origin of pegnology. Advanced drug delivery reviews. 2002;54(4):457-8.
108. Bollinger ME, Arredondo-Vega FX, Santisteban I, Schwarz K, Hershfield MS, Lederman HM. Hepatic dysfunction as a complication of adenosine deaminase deficiency. New England Journal of Medicine. 1996;334(21):1367-72.
109. Noël A, Jost M, Lambert V, Lecomte J, Rakic J-M. Anti-angiogenic therapy of exudative age-related macular degeneration: current progress and emerging concepts. Trends in molecular medicine. 2007;13(8):345-52.
110. Almeida AJ, Souto E. Solid lipid nanoparticles as a drug delivery system for peptides and proteins. Advanced drug delivery reviews. 2007;59(6):478-90.
111. Molineux G. The design and development of pegfilgrastim (PEG-rmetHuG-CSF, Neulasta®). Current pharmaceutical design. 2004;10(11):1235-44.
112. Griffin M, Salmasi S, Naderi N, Butler PE, Seifalian AM. Advancing Translational Nanotechnology to Clinical Application. Stem Cell Nanoengineering. 2014:365.
113. Avramis VI, Sencer S, Periclou AP, Sather H, Bostrom BC, Cohen LJ, et al. A randomized comparison of nativeEscherichia coli asparaginase and polyethylene glycol conjugated asparaginase for treatment of children with newly diagnosed standard-risk acute lymphoblastic leukemia: a Children's Cancer Group study. Blood. 2002;99(6):1986-94.
114. Gref R, Minamitake Y, Peracchia MT, Trubetskoy V, Torchilin V, Langer R. Biodegradable long-circulating polymeric nanospheres. Science. 1994;263(5153):1600-3.
115. Torchilin VP. Micellar nanocarriers: pharmaceutical perspectives. Pharmaceutical research. 2007;24(1):1-16.

116. Tobio M, Gref R, Sanchez A, Langer R, Alonso M. Stealth PLA-PEG nanoparticles as protein carriers for nasal administration. Pharmaceutical research. 1998;15(2):270-5.
117. Perez C, Sanchez A, Putnam D, Ting D, Langer R, Alonso M. Poly (lactic acid)-poly (ethylene glycol) nanoparticles as new carriers for the delivery of plasmid DNA. Journal of controlled Release. 2001;75(1):211-24.
118. Farokhzad OC, Cheng J, Teply BA, Sherifi I, Jon S, Kantoff PW, et al. Targeted nanoparticle-aptamer bioconjugates for cancer chemotherapy in vivo. Proceedings of the National Academy of Sciences. 2006;103(16):6315-20.
119. Kabanov AV, Batrakova EV, Alakhov VY. Pluronic® block copolymers as novel polymer therapeutics for drug and gene delivery. Journal of controlled release. 2002;82(2):189-212.
120. Langer R, Tirrell DA. Designing materials for biology and medicine. Nature. 2004;428(6982):487-92.
121. Edelman ER, Mathiowitz E, Langer R, Klagsbrun M. Controlled and modulated release of basic fibroblast growth factor. Biomaterials. 1991;12(7):619-26.
122. Langer R, Folkman J. Polymers for the sustained release of proteins and other macromolecules. 1976.
123. Langer R. Drug delivery and targeting. Nature. 1998;392(6679 Suppl):5-10.
124. Hafner A, Lovrić J, Lakoš GP, Pepić I. Nanotherapeutics in the EU: an overview on current state and future directions. International journal of nanomedicine. 2014;9:1005.
125. Torchilin VP. Recent advances with liposomes as pharmaceutical carriers. Nature reviews Drug discovery. 2005;4(2):145-60.
126. Mozafari MR. Liposomes: an overview of manufacturing techniques. Cellular and Molecular Biology Letters. 2005;10(4):711.
127. Vyas SP, Khar RK. Targeted & Controlled Drug Delivery: Novel Carrier Systems: CBS publishers & distributors; 2004.
128. Lasic DD. The mechanism of vesicle formation. Biochemical Journal. 1988;256(1):1.
129. Olson F, Hunt C, Szoka F, Vail W, Papahadjopoulos D. Preparation of liposomes of defined size distribution by extrusion through polycarbonate membranes. Biochimica et Biophysica Acta (BBA)-Biomembranes. 1979;557(1):9-23.

130. Sharma A, Sharma US. Liposomes in drug delivery: progress and limitations. International journal of pharmaceutics. 1997;154(2):123-40.
131. Tyrrell D, Heath T, Colley C, Ryman BE. New aspects of liposomes. Biochimica et Biophysica Acta (BBA)-Reviews on Biomembranes. 1976;457(3):259-302.
132. Pick U. Liposomes with a large trapping capacity prepared by freezing and thawing of sonicated phospholipid mixtures. Archives of biochemistry and biophysics. 1981;212(1):186-94.
133. Kasahara M, Hinkle PC. Reconstitution and purification of the D-glucose transporter from human erythrocytes. Journal of Biological Chemistry. 1977;252(20):7384-90.
134. KALEPU S, SUNILKUMAR K, BETHA S. Liposomal drug delivery system-A Comprehensive Review. Int J Drug Dev & Res. 2013;5(4):0975-9344.
135. Szoka F. Liposomal drug delivery: current status and future prospects. Marcel Dekker, New York; 1991. p. 845-90.
136. Gregoriadis G. Engineering liposomes for drug delivery: progress and problems. Trends in biotechnology. 1995;13(12):527-37.
137. Lasic D, Papahadjopoulos D. Liposomes revisited. Science. 1995;267(5202):1275.
138. Torchilin V. Liposomes as targetable drug carriers. Critical reviews in therapeutic drug carrier systems. 1984;2(1):65-115.
139. Simões S, Moreira JN, Fonseca C, Düzgüneş N, de Lima MCP. On the formulation of pH-sensitive liposomes with long circulation times. Advanced drug delivery reviews. 2004;56(7):947-65.
140. Yuan F, Leunig M, Huang SK, Berk DA, Papahadjopoulos D, Jain RK. Mirovascular permeability and interstitial penetration of sterically stabilized (stealth) liposomes in a human tumor xenograft. Cancer research. 1994;54(13):3352-6.
141. Gabizon A, Papahadjopoulos D. Liposome formulations with prolonged circulation time in blood and enhanced uptake by tumors. Proceedings of the National Academy of Sciences. 1988;85(18):6949-53.
142. Klibanov AL, Maruyama K, Torchilin VP, Huang L. Amphipathic polyethyleneglycols effectively prolong the circulation time of liposomes. FEBS letters. 1990;268(1):235-7.
143. Blume G, Cevc G. Molecular mechanism of the lipid vesicle longevity in vivo. Biochimica et Biophysica Acta (BBA)-Biomembranes. 1993;1146(2):157-68.

144. Torchilin VP, Omelyanenko VG, Papisov MI, Bogdanov AA, Trubetskoy VS, Herron JN, et al. Poly (ethylene glycol) on the liposome surface: on the mechanism of polymer-coated liposome longevity. Biochimica et Biophysica Acta (BBA)-Biomembranes. 1994;1195(1):11-20.

145. Torchilin VP, Trubetskoy VS. Which polymers can make nanoparticulate drug carriers long-circulating? Advanced drug delivery reviews. 1995;16(2):141-55.

146. Maeda H, Sawa T, Konno T. Mechanism of tumor-targeted delivery of macromolecular drugs, including the EPR effect in solid tumor and clinical overview of the prototype polymeric drug SMANCS. Journal of controlled release. 2001;74(1):47-61.

147. Whiteman K, Subr V, Ulbrich K, Torchilin V. Poly (HPMA)-coated liposomes demonstrate prolonged circulation in mice. Journal of Liposome Research. 2001;11(2-3):153-64.

148. Torchilin V, Levchenko T, Whiteman K, Yaroslavov A, Tsatsakis A, Rizos A, et al. Amphiphilic poly-N-vinylpyrrolidones:: synthesis, properties and liposome surface modification. Biomaterials. 2001;22(22):3035-44.

149. Takeuchi H, Kojima H, Yamamoto H, Kawashima Y. Evaluation of circulation profiles of liposomes coated with hydrophilic polymers having different molecular weights in rats. Journal of Controlled Release. 2001;75(1):83-91.

150. Fattal E, Couvreur P, Dubernet C. "Smart" delivery of antisense oligonucleotides by anionic pH-sensitive liposomes. Advanced drug delivery reviews. 2004;56(7):931-46.

151. Asokan A, Cho MJ. Cytosolic delivery of macromolecules: II. Mechanistic studies with pH-sensitive morpholine lipids. Biochimica et Biophysica Acta (BBA)-Biomembranes. 2003;1611(1):151-60.

152. Roux E, Passirani C, Scheffold S, Benoit J-P, Leroux J-C. Serum-stable and long-circulating, PEGylated, pH-sensitive liposomes. Journal of controlled release. 2004;94(2):447-51.

153. Turk MJ, Reddy JA, Chmielewski JA, Low PS. Characterization of a novel pH-sensitive peptide that enhances drug release from folate-targeted liposomes at endosomal pHs. Biochimica et Biophysica Acta (BBA)-Biomembranes. 2002;1559(1):56-68.

154. Gabizon AA. Pegylated liposomal doxorubicin: metamorphosis of an old drug into a new form of chemotherapy. Cancer investigation. 2001;19(4):424-36.

155. Allen T, Hansen C. Pharmacokinetics of stealth versus conventional liposomes: effect of dose. Biochimica et Biophysica Acta (BBA)-Biomembranes. 1991;1068(2):133-41.
156. Blomme S. Toxicological Evaluation of Liposomal Antimicrobials: ProQuest; 2008.
157. Grit M, Crommelin DJ. Chemical stability of liposomes: implications for their physical stability. Chemistry and physics of lipids. 1993;64(1):3-18.
158. Chao F-F, Blanchette-Mackie E, Tertov V, Skarlatos S, Chen Y, Kruth H. Hydrolysis of cholesteryl ester in low density lipoprotein converts this lipoprotein to a liposome. Journal of Biological Chemistry. 1992;267(7):4992-8.
159. Klein R. The detection of oxidation in liposome preparations. Biochimica et Biophysica Acta (BBA)-Lipids and Lipid Metabolism. 1970;210(3):486-9.
160. Mayer L, Bally M, Cullis P. Uptake of adriamycin into large unilamellar vesicles in response to a pH gradient. Biochimica et Biophysica Acta (BBA)-Biomembranes. 1986;857(1):123-6.
161. Clerc S, Barenholz Y. Loading of amphipathic weak acids into liposomes in response to transmembrane calcium acetate gradients. Biochimica et Biophysica Acta (BBA)-Biomembranes. 1995;1240(2):257-65.
162. Sharma A, Straubinger RM. Novel taxol formulations: preparation and characterization of taxol-containing liposomes. Pharmaceutical research. 1994;11(6):889-96.
163. Lee KY, Mooney DJ. Hydrogels for tissue engineering. Chemical reviews. 2001;101(7):1869-80.
164. Hutmacher DW. Scaffold design and fabrication technologies for engineering tissues—state of the art and future perspectives. Journal of Biomaterials Science, Polymer Edition. 2001;12(1):107-24.
165. Huang X, Brazel CS. On the importance and mechanisms of burst release in matrix-controlled drug delivery systems. Journal of controlled release. 2001;73(2):121-36.
166. Wei J, Chen F, Shin J-W, Hong H, Dai C, Su J, et al. Preparation and characterization of bioactive mesoporous wollastonite–polycaprolactone composite scaffold. Biomaterials. 2009;30(6):1080-8.
167. Richardson TP, Peters MC, Ennett AB, Mooney DJ. Polymeric system for dual growth factor delivery. Nature biotechnology. 2001;19(11):1029-34.

168. Lehár J, Krueger AS, Avery W, Heilbut AM, Johansen LM, Price ER, et al. Synergistic drug combinations tend to improve therapeutically relevant selectivity. Nature biotechnology. 2009;27(7):659-66.

169. Hennink W, Van Nostrum CF. Novel crosslinking methods to design hydrogels. Advanced drug delivery reviews. 2012;64:223-36.

170. Glotzer SC, Solomon MJ. Anisotropy of building blocks and their assembly into complex structures. Nature materials. 2007;6(8):557-62.

171. Numata K, Yamazaki S, Naga N. Biocompatible and biodegradable dual-drug release system based on silk hydrogel containing silk nanoparticles. Biomacromolecules. 2012;13(5):1383-9.

172. Grijalvo S, Mayr J, Eritja R, Díaz DD. Biodegradable liposome-encapsulated hydrogels for biomedical applications: a marriage of convenience. Biomaterials science. 2016.

173. Thirumaleshwar S, K Kulkarni P, V Gowda D. Liposomal Hydrogels: A novel drug delivery system for wound dressing. Current Drug Therapy. 2012;7(3):212-8.

174. Chen F-M, Zhang M, Wu Z-F. Toward delivery of multiple growth factors in tissue engineering. Biomaterials. 2010;31(24):6279-308.

175. King WJ, Krebsbach PH. Growth factor delivery: how surface interactions modulate release in vitro and in vivo. Advanced drug delivery reviews. 2012;64(12):1239-56.

176. Ehrick JD, Deo SK, Browning TW, Bachas LG, Madou MJ, Daunert S. Genetically engineered protein in hydrogels tailors stimuli-responsive characteristics. Nature materials. 2005;4(4):298-302.

177. Kopeček J. Polymer chemistry: swell gels. Nature. 2002;417(6887):388-91.

178. Tang Y, Zhao Y, Li Y, Du Y. A thermosensitive chitosan/poly (vinyl alcohol) hydrogel containing nanoparticles for drug delivery. Polymer bulletin. 2010;64(8):791-804.

179. Gao W, Vecchio D, Li J, Zhu J, Zhang Q, Fu V, et al. Hydrogel containing nanoparticle-stabilized liposomes for topical antimicrobial delivery. ACS nano. 2014;8(3):2900-7.

Chapter 2 : Release Kinetics of Nano-Inclusion Based and Affinity Based Hydrogels: A Comparative Study

S. Alsharif [a], P-L. Latreille [a], O. Gourgas [b], S.F. Tehrani [b], X. Banquy [a], and V.G. Roullin [b]

Authors contribution :

S. Alsharif [a] : Performed experiments and results analysis on liposomes, hydrogels and nanogels.

P-L. Latreille [a] : Performed experiments and results analysis on microgels and hydrogels. Compared release profiles between diffusion-based and affinity-based systems.

O. Gourgas [b] : Designed hydrogel synthesis protocol.

S.F. Tehrani [b] : Participated in microgels preparation and characterization.

X. Banquy [a] : Supervisor.

V.G. Roullin [b] : Supervisor.

2.1. Introduction

Over the past two decades, significant advancements have occurred in the field of nanotechnology led to nano-scale particles whose physical and chemical properties are beneficial to therapeutic purposes (1). Most nanoparticle technologies involved in therapeutic applications have been found to be advantageous for controlled delivery systems of active compounds. Nanoparticles are made from either naturally sourced material or synthetic polymers. Natural sources are typically phospholipids, lipids, natural polymers such as chitosan, while as synthetic nanoparticles can be fabricated from polylactic acid (2), polycaprolactone (PCL), polylactic-co-glycolic acid (PLGA) or microgels (acrylate based polymers) (3-6). However, optimizing carriers for active compound delivery is a question of active compound use, encapsulation and release, shelf life stability, biocompatibility, biodistribution and functionality (7, 8). In addition, when different materials used for developing carriers, possible side effects from residual materials after active compounds delivery that should be concerned. So, biodegradable nanocarriers with optimized half-life would be most practical for therapeutic use (9).

The main goal of active compound encapsulation is to improve delivery to, or uptake by, target tissues or to minimize the toxicity of the free active compounds to non-target tissues (10). An improvement in either of the properties leads to an increase in therapeutic index, that is, the margin between the doses resulting in a therapeutic efficacy and toxicity to other tissues. Thus, developing a long-acting nanocarrier is of interest. Nevertheless, the criteria for choosing the appropriate nanocarrier most frequently depends on the active compound's potency, stability, solubility, charge, and molecular weight. Generally, finely designed nanocarriers, such as liposomes, are able to encapsulate only a small amount of active compound molecules. Mainly, high potency active compounds are usually encapsulated in practice (11). Since Alec Bangham discovered liposomes 40 years ago, they have gained an interest and have been involved in medical and pharmaceutical research as a fundamental tool in controlled active compound delivery systems (12). Another type of nanocarrier that has

recently attracted attention as an efficient polymeric based drug delivery system is nanogels. They have demonstrated flexibility in their capacity for both active compounds encapsulation and release. As such, there is a room to improve the encapsulation rate of a variety of active compounds (13). Nanogels can be modified to respond to environmental changes to facilitate spatial and temporal controlled release in physiological conditions (14). In this study, we have employed chitosan-based nanogels because of their bioactivity, biodegradability and biocompatibility properties that make them optimal for *in vivo* applications (15). Chitosan is a natural polyelectrolyte, β (1→4)-linked linear copolymer of 2-amino-2-deoxy-β-d-glucan (GlcN) and 2-acetamido-2-deoxy-β-d-glucan (GlcNAte). Conformation and resulting characteristics of chitosan rely on different physicochemical parameters (16-20). Also, chitosan was found to be advantageous in terms of active compounds delivery and regenerative medicine (21, 22).

The thermo-sensitivity and pH sensitivity of nanocarriers could be manipulated to control the release, or trigger the release, of active compounds (23-25). NIPAM microgels were first reported by Pelton and Chibante in 1986 (26). Microgels can be made from N-isopropylacrylamide (NIPAM) where pNIPAM is a thermo-sensitive polymer that can be co-polymerized with a charged monomer to provide pH-sensitivity. The authors polymerized NIPAM with N,N'-methylene-bis(acrylamide) (bisAc) in water to produce micro-scaled latexes sensitive to temperature. These particles have the capability to swell below the lower critical solubility temperature (LCST) of NIPAM, at approximately 32°C, while it is capable of collapsing and decreasing their sizes above the LCST (27). Since then, this effect has been widely characterized and it was found possible to finely tune the LCST and electrical charge of the microgels to adequately respond to pH or temperature changes in specified range (28). Furthermore, electrical charges within the polymer structure might enhance the encapsulation of a drug within the microgel as well as control its release through electrostatic interaction between the microgel and a charged active compound. No organic solvents are used for the synthesis; it is produced in one scalable step synthesis and the size, size variation, surface properties and monomer composition can be modified to adjust the microgel for specific therapeutic applications (29, 30).

Invasive administration methods would benefit from sustained release, which could reduce dosage frequency. For example, implants, drug loaded patches and tissue design platforms are potential applications but require a biocompatible polymeric matrix to entrap nanocarriers capable of sustaining and controlling the release of the active compounds (31, 32).

Synergistic combination of different carriers as a novel controlled delivery system has attracted attention due to its potential for administrating different active compounds while also providing better controlled release rate. Consequently, minimized side effects and improved therapeutic profiles can be achieved with lower dosage requirements (33). Synergistic controlled delivery systems are currently fabricated with hydrogel embedding either polymers or lipid based nanoparticles (9, 33-35).

A hydrogel with high water content was designed to represent biocompatible or tissue mimicking synthetic matrices for embedding nanocarriers. We have evaluated the capabilities of liposomes, nanogels, and microgels nanocarriers embedded in acrylamide/bisAc polymeric matrix as a generic matrix. The objective is to evaluate the potential in controlling the release of a model active compound from a three-dimensional matrix embedding different nanocarriers separately and evaluating the impact of temperature, medium salinity and composition of each nanocarrier. In this study, the comparison between three different nanocarriers embedded within a hydrogel should help elucidate the different release mechanisms and how the structure influences the release behaviour of each formulation.

2.2. Materials and methods

2.2.1. Chemicals and reagents

Phospholipids including 1,2-Dioleoyl-sn-glycero-3-phosphocholine (DOPC) and 1,2-dihexadecanoyl-sn-glycero-3-phosphocholine (DPPC) were purchased from Avanti Polar Lipids (USA) and used without further purification. For liposome preparation, Kiton Red S (Sulforhodamine B) was purchased from Alfa Aesar (Ward Hill, MA, USA). Surfactant triton X-100 provided by Sigma–Aldrich was used for the release kinetics measurement. Sephadex G-50 from Sigma was used to separate liposomes from non-encapsulated sulforhodamine B solution. For nanogels preparation, chitosan (Mw= 88 kDa) derived from shrimp shells was purchased from Sigma (France). Hyaluronic acid sodium salt (Mw = 1 400 kDa) was extracted from Streptococcus equi subspecies (Sigma-Aldrich, France) and used as received. Sodium tripolyphosphate (TPP) was purchased from Alfa Aesar (Ward Hill, MA, USA). Citric acid was purchased from Anachemia (Canada). The microgel was prepared from N-Isopropylacrylamide (NIPAM), N,N'-methylene-bis(acrylamide) (BisAc), methacrylic acid (12) and sodium dodecyl sulfate (SDS) which were provided by Sigma-Aldrich (Canada). Ammonium persulfate initiator was provided by Fisher-Biotech (Canada). To prepare the hydrogel, Acrylamide (AAm) monomer and N,N'-methylene-bis(acrylamide) (BisAc) cross-linker were purchased from Sigma-Aldrich (Canada) and Irgacure ® 2959 as photoinitiatior was supplied by BASF (Switzerland). HEPES buffer from Sigma–Aldrich was used for hydrogel preparation and analysis

2.2.2. Preparation of formulations

2.2.2.1. Liposome preparation

The preparation of liposome was started by dissolving of 20 mg of a (DOPC:DPPC) mixture at the required ratio in 1 mL of chloroform in order to prepare three different batches with phospholipids molar ratios of (50:50), (60:40), and (70:30) of DOPC:DPPC. Then, the solvent was slowly removed by rotary evaporation under

reduced pressure at 50℃ to form a thin lipid film in a 10 mL round bottom flask. The lipid film was further dried by freeze-drying for 15 minutes to eliminate the residual solvent content. 1 mL of 30 mM sulforhodamine B in a buffer of 5 mM HEPES and 145 mM NaCl was added to the flask to hydrate the lipid film. This process was performed at 60℃ while mixing and vortexing for 20 minutes until all the phospholipids were hydrated and removed from the flask wall. The dispersion was then treated by 10 freeze-thaw cycles followed by 21 cycles of extrusion (Avanti Mini-Extruder; Avanti Polar Lipids, USA) through a polycarbonate membrane with a pore size of 200 nm and by the same process in a 100 nm membrane in order to approach small monodisperse unilamellar liposomes. Non-encapsulated sulforhodamine B was separated from liposomes by size exclusion chromatography using 1 x 20 cm Sephadex G-50 (medium) column equilibrated in a pH 7.4 buffer (5 mM HEPES and 145 mM NaCl). After that, purified liposomes with final total volume of ~ 3 mL were collected and stored in darkness at 4°C in 4 mL glass vials for later tests.

2.2.2.2. Chitosan nanogel preparation and drug loading

For the nanogel, chitosan (CS) and hyaluronic acid (HA) were chosen as polymeric matrix for biocompatibility reasons. The cationic character of chitosan in acidic solution allows electrostatic interactions with negatively charged small molecules or polymers to form nanoparticulate complexes through ionic gelation (36). CS was solubilized in 9 mL of 10 % (w/v) citric acid aqueous solution at concentration of 2.5 mg/mL under magnetic stirring for 45 minutes until full dissolution. Next, the CS solution was filtered using a 0.2 µm nylon membrane filter (Ultident Scientific, Canada). A solution of TPP 1.2 mg/mL and HA 0.8 mg/mL was prepared in 4.5 mL milli-Q water under magnetic stirring until full dissolution. The solution was also filtered by 0.2 µm nylon membrane filter as same as in CS.

Sulforhodamine B at a concentration of 4 mg/mL was then added to the TPP/HA solution under magnetic stirring for 15 minutes. Chitosan-based nanogels were formed spontaneously during dropwise addition of 4.5 mL of the TPP / HA solution to 9 mL of CS solution under ultrasonication (Fischer Scientific Sonic Dismembrator F550 Ultrasonic

Homogenizer; power sonicator 20%) on an ice bath for 90 seconds. The formation of inter- and intramolecular electrostatic-mediated cross-linking among polyanions and protonated CS chains induced the gelation process (35). Once the dropwise addition was finished, continuous magnetic stirring was maintained for 20 minutes. The resulting loaded nanogels were stored at 4°C and protected from light exposure. A volume of 12 mL of loaded nanogel suspensions were purified three times at room temperature using 1.2 L of 5 mM HEPES buffer by tangential flow filtration using MicroKros® hollow fiber modules (Spectrum, MicroKros® ME, MWCO 0.05 µm) in order to remove citric salts and the non-encapsulated sulforhodamine B.

2.2.2.3. NIPAM-co-MAA microgel preparation

Thermosensitive microgels were prepared in order to include anionic charges at different concentrations (provided by MAA co-monomer) within the NIPAM structure. The synthesis of the NIPAM-co-MAA particles was carried out in a single step. NIPAM and MAA were dissolved in degassed milliQ water at different molar ratios (molMAA / [molNIPAM + molMAA]) (30, 37-39). NIPAM and MAA were dissolved in degassed milliQ water at different molar ratios (molMAA / [molNIPAM + molMAA]), (table 2.1). BisAc at 5% molar ratio of total monomers and cross-linker in the particle and SDS at 867 µmol/L were added to the degassed solution. The contents were stirred until complete homogenization. A total of 150 mL of monomer/cross-linker/surfactant solution was transferred into a three necked flask heated under reflux at approximately 60^{o}C with constant Argon gas flow and mechanical stirring (275 rpm). The reaction was initiated with the addition of 10 mL APS (solution at 2.9 mmol/L) degassed by vacuum, while slowly increasing temperature to 75°C, maintaining steady Argon flow rate and mechanical stirring speed. The reaction was stopped after 4.5 hours by cooling down the particle suspension and removing large aggregates if any. The microgels were purified in batches of 60-70 mL by two consecutive dynamic dialysis in 20 L milliQ water for 16 hours and 4 hours respectively, using Spectra/Por® Tube-A-Lyzer® (Rancho Dominguez, USA) a

dynamic dialysis device with 100 kD MWCO cellulose ester membrane. Microgel suspensions were stored at 4℃ until use.

2.2.2.4. Hydrogel preparation

Hydrogels were prepared by free radical photopolymerization of acrylamide (AAm) as the monomer, and N-N'-methylene-bisacrylamide (BisAc) as a cross-linker in HEPES buffer (pH 7.4) with cross-linker:monomer molar ratio of (5% w/v) (40). The cross-linker/monomer solution was prepared by dissolution of 1.90 g of AAm and 100 mg BisAc in 20 mL of 5 mM HEPES and 145 mM NaCl under magnetic stirring. This stock solution was frozen at – 80°C for 1 hour. Before the polymerization process, the cross-linker/monomer solution was degassed using a vacuum pump for 30 minutes to eliminate dissolved oxygen that would otherwise prevent free radical photopolymerization. Following that, the solution was incubated in a water bath at 32°C for 20 minutes. 2 mL of the solution was then collected into 10 mL glass beaker where the photopolymerization process takes place.

A solution of photoinitiator was added to an initiator/total monomer molar ratio of 5% in the final gel in order to start the reaction. Under magnetic stirring, the initiator solution was prepared by dissolving 5.8 mg of Irgacure® 2959 in 2 mL of HEPES buffer that had been already frozen, degassed and thawed. 300 µL of initiator solution were added to the reaction mixture within the beaker. Liposomes were introduced into the hydrogels by diluting purified liposome suspensions in the reactive medium of hydrogel synthesis.

For hydrogel preparation embeded with R6G-loaded microgels, each hydrogel was prepared separately. 190 mg AAm and 10 mg BisAc were dissolved in R6G-loaded microgel suspension (volume determined by drug loading) and the volume was adjusted with HEPES 5 mM without salt or milliQ water (depending on R6G loading medium) to reach the same AAm /BisAc concentration prior to the addition of Irgacure® 2959.

The photocrosslinked hydrogels were obtained by exposing the 10 ml beaker containing the mixture to a UV lamp (365 nm; High Intensity UV Lamp; 40 min exposure). The beaker was covered with a glass slide to prevent evaporation. After photopolymerization, hydrogels of 5 mm diameter and thickness of ~ 5 mm disks were cut out using a biopsy punch (Miltex ®) for release study.

2.2.3. Physicochemical characterization of formulations

The size of liposomes and nanogels were measured using dynamic light scattering (DLS) from a Malvern Zetasizer NanoZS (Malvern Instruments, UK), which were calculated from the Z-averages of the hydrodynamic diameters (dH, Z) and polydispersity indexes (PdI). Each sample was analysed in triplicate at 25°C. Water and water-citric acid (0.48 M) mixtures were used as reference dispersing media for liposomes and nanogels respectively. The size of each microgel suspension was determined as a function of temperature to characterize its thermo-sensitivity. Measurement started from 20°C, with 2°C increments between each measurement, up to 40°C in milliQ water, phosphate buffed saline at pH 7.4 (PBS) and HEPES 5mM without salts at pH 7.4. Zeta potential data were measured by electrophoretic light scattering (ELS) at 25°C, 150 V, in triplicate for each sample (Malvern Zetasier Nano-ZS) in MilliQ water for liposomes and nanogels. The microgel zeta potentials were measured in 4 mM NaCl medium at 22°C and 38°C.

2.2.4. Determination of loading efficiency (LE%) and drug loading (DL%)

2.2.4.1. Liposome

In order to determine the DL% for each liposome formulation, the Bartlett method was performed for each formulation following their purification to quantify inorganic phosphate in phospholipids, which will be used to calculate the recovered concentration of liposome phospholipids (41). Then, certain volume was collected into quartz cuvette from each formulation dispersed in 5 mM HEPES and 145 mM NaCl buffer (pH 7.4) with final volume of 3000 µl containing fixed concentration of liposomes of 15 µM loaded with sulforhodamine B. The amount of loaded

sulforhodamine B in the liposomes was determined by spectrofluorimetry (Hitachi F-2710 fluorescence spectrophotometer) after addition of 10 µl of Triton X-100 while heating at 65°C and stirring for 10 minutes, resulting in liposomes permeation and release their content totally until no further increase in intensity was noticed. Then, 100 µL of suspension was collected and further diluted 10 times in 5 mM HEPES and 145 mM NaCl to fit a linear concentration range. Sulforhodamine B intensity was measured under stirring at maximum emission wavelength of 582 nm after excitation of samples at 563 nm. The excitation and emission slits were fixed at 5 nm for all measurements. Fluorescence intensity of diluted sulforhodamine B from each formulation was found to be linearly proportional to sulforhodamine B concentrations ranging from 0.005 µM to 1µM. After that, the total quantity (adjusted for dilution factor) of sulforhodamine B released was calculated based on the concentration obtained from the calibration curve. The quantities of loaded sulforhodamine B in the stock formulations were also calculated. Following that, sulforhodamine B loading efficiency (LE%) and drug loading (DL%) of liposomes were calculated as:

$$LE\% = \frac{Drug_{loaded}}{Drug_{total}} \times 100 \quad \text{(Eq. 2.1)}$$

$$DL\% = \frac{Drug_{loaded}}{M_{Np}} \times 100 \quad \text{(Eq. 2.2)}$$

$Drug_{loaded}$ is the amount of model drug loaded in nanoparticles, $Drug_{total}$ is the total amount of model drug used in the preparation, and M_{Np} is the total mass of obtained nanoparticles for every formulation.

2.2.4.2. Nanogels

Following the preparation of sulforhodamine B loaded nanogels, 500 µL from the batch was collected and centrifuged at 20000 rpm for 20 minutes in order to separate nanogels from the aqueous suspension. Then, 100 µL of the supernatant was collected and diluted 100 times in 5 mM HEPES buffer to fit the calibration curve. The

amount of free sulforhodamine in the supernatant (djusted for dilution factor) was determined by a spectrofluorimetry (Tecan Safire Monochromatic Fluorescence). The sulforhodamine B intensity was measured at maximum emission wavelength of 582 nm after excitation of samples at 563 nm. The excitation and emission slits were fixed at 5 nm. Fluorescence intensity of diluted supernatant was found to be linearly proportional to sulforhodamine B concentrations ranging from 0.005 µM to 1µM. The sulforhodamine B loading efficiency (LE%) and drug loading (DL%) of nanogels were calculated using Eq. 2.1 and Eq. 2.2.

2.2.4.3. NIPAM-co-MAA microgels

Microgel concentration in the stock solution was determined by freeze-drying after purification, and then weighting the residual polymer in triplicate. A fluffy white powder remains in the tubes allowing for easy mass measurement. Microgel suspensions were loaded using R6G positively charged fluorescent dye. Since microgels of NIPAM-co-MAA are negatively charged, drug loading ocurred through electrostatic interaction. A stock solution of 0.5 mg/mL R6G was prepared in milliQ water and kept at 4°C until use. The stock microgel suspension was diluted in milliQ water to reach a concentration of 0.5 mg/mL. 100 µL of diluted microgels were transferred, and different concentrations of R6G were used to load the microgels (0.2, 0.4, 0.6, 0.8 mg/mL) and topped with milliQ water to 500 µL. HEPES 5 mM with 145 mM NaCl (pH 7.4) and HEPES 5 mM (pH 7.4) without salt were used for calculating drug loading and loading efficiency. The suspension was vortexed and then incubated for 1 hour at different temperatures 25°C and 40°C. Temperature cycling was tested in order to verify if swelling / shrinking cycles could improve R6G loading. The sample started incubation in the swollen state at 0°C or 25°C for 20 minutes then was heated to 40°C for 20 minutes then returned to the initial temperature for the last 20 minutes. At the end of the incubation process, the drug-loaded microgels were centrifuged at 25000 G for 30 minutes. The supernatant was collected, then diluted 20 times and transferred to a 96-well plate for fluorescence measurement. Fluorescence of the diluted supernatant was determined by spectrofluorimetry (Tecan Safire Monochromatic Fluorescence) and concentration was

determined using a linear calibration curve between 10 and 0.25 µg/mL. Each parameter in this study was assessed in triplicate and measured independently three times (n= 3). DL% and LE% were calculated using Eq. 2.1 and Eq. 2.2.

2.2.4.4. Drug loading for drug release using NIPAM-co-MAA microgels

In order to obtain a sufficient quantity of loaded R6G, the loading volume for each microgel suspension was 90 mL using milliQ water. A total of 30 mL was used for 10, 12.5, 15, 20% MAA and 90 mL was used for 5% MAA in HEPES 5 mM without a salt medium. R6G concentration was set to 0.06 mg/mL and the microgel concentration was set to 0.1 mg/mL. The suspension was then incubated at 25°C for 1 hour. Two cycles of centrifugation and re-suspension of the microgels were performed to remove free R6G. Centrifugation was carried out at 30000 G for 1 hour at 4°C using Sorvall RC-6 (Thermo-Scientific) and Rotor SS-34 centrifuges. Re-suspension occurred in the same volume and incubation medium. 1 mL of milliQ water or HEPES 5mM without salt was used to re-suspend the remaining microgel at the end of the centrifugation process. To evaluate the concentration of encapsulated R6G, 20 µL was collected from the suspension and was diluted 200 times in HEPES buffer (containing salt). DL% and LE% were calculated using Eq. 2.1 and Eq. 2.2. The concentration of microgels was determined after freeze-drying.

2.2.5. Release study from liposomes

Release from suspended liposomes was performed as a function of liposomal concentration, composition and temperature. The release profile of sulforhodamine B from liposomes was measured and evaluated by conventional fluorescence for three different formulations (50:50, 60:40, and 70:30) separately over 72 hours at 4°C and 37°C. Sulforhodamine B intensity was measured using a spectrophotometer (Hitachi F-2710 fluorescence spectrophotometer) while stirring at the maximum emission wavelength of 582 nm and excitation wavelength of 563 nm. The excitation and emission slits were fixed at 5 nm for all measurements.

Two samples were collected from the stock of every loaded liposome formulation and dispersed separately in 5 mM HEPES and 145 mM NaCl (pH 7.4) up to a final volume of 3000 µL and total liposomes concentration of 15 µM. After mixing and pouring into 20 ml glass vials, one set from each formulation was stored under darkness at 4°C while the other set was incubated under darkness at 37°C. The samples for each formulation (50:50, 60:40, and 70:30) incubated at 4°C and 37°C were separately collected into quartz cuvettes, where fluorescence intensities were measured while stirring at regular time intervals over 72 hours. To obtain maximum sulforhodamine B release and intensity, 10 µL of Triton X-100 was added and stirred for 10 minutes while heating at 65°C. resulting in liposomes permeation and release their content totally.

Based on calibration curve between 0.024 µM and 4.8 µM, fluorescence intensities of released sulforhodamine B during different time intervals and after obtaining the maximum release (using Triton X-100) were used to calculate the released concentrations. The release percentage was calculated from the concentrations of sulforhodamine B released during time intervals and maximum released concentrations of sulforhodamine B after liposomes permeation.

2.2.6. Release study from hydrogel

During hydrogel synthesis, the loaded liposomes were added to the reactive mixture of hydrogels. The photopolymerization process yielded hydrogels with embedded liposomes loaded with 0.27 mg of sulforhodamine B. Then, hydrogels were cut into 5 mm diameter and thickness cylinders and their masses were measured in order to estimate the sulforhodamine B mass content in every cylinder, assuming that the solution mixture is homogenous. The same process was repeated for nanogels. Hydrogel discs 5 mm diameter and thickness of 5 mm were separately placed in 10 mL of 5 mM HEPES buffer (pH 7.4) at 4°C and 37°C. After that, at different time intervals, 200 µL of the supernatant was taken (and replaced by 200 µL of fresh HEPES buffer) and analysed by spectrofluorimetry (Tecan Safire Monochromatic Fluorescence). The release study was performed in triplicate (n= 3) over 240 hours for

liposomes and 72 hours for nanogels respectively. The percentage of released sulforhodamine B was calculated relative to the estimation of the maximum sulforhodamine B concentration that could be released. Release studies using microgels embedded in hydrogels was performed using R6G instead of sulforhodamine B. From the medium, 300 μL was collected and replaced by the same volume with fresh HEPES buffer. R6G released from the microgel embedded in AAm/BisAc was investigated over 72 hours.

2.3. Results and Discussions

2.3.1. Preparation and characterization of liposomes

Three formulations with different phospholipids molar ratios (50:50, 60:40, and 70:30) were prepared in order to identify the effect of liposome concentration over particle size and zeta potential (table 2.1). Increasing DOPC concentration in the liposome had a limited effect on changing the hydrodynamic diameters among all formulations with a stable PDI value of 0.1. However, ZP values were found to increase significantly from -24.03±4 mV in 50:50 formulation to -60.7±1.6 mV along with the increase in DOPC. Results (table 2.1) showed that the highest DL (40%) and LE (8%) were obtained in the formulation containing equal ratios of DOPC:DPPC, while the lowest DL (12%) and LE (1%) were obtained from the DOPC:DPPC (70:30) formulation. These findings suggest that 50:50 formulation is best to achieve optimal sulforhodamine B loaded liposomes because of higher encapsulation rates associated with higher DPPC content, which prevents loaded molecules from leaking out. The variations in DL and LE are due to the change in the liposome membrane fluidity, which depends on differences in both the phospholipid composition and temperature. Since DOPC and DPPC have transition temperatures of -21°C and 41°C, representing mobile phase and solid phase respectively and due to presence of double bonds in the DPOC acyl chain, the increase in the DOPC:DPPC provided liposomes with higher bilayers membrane fluidity. As a result, the liposomes with higher DOPC composition (60:40, 70:30) were not capable of encapsulating the same amount of sulforhodamine B compared to liposomes with higher DPPC (50:50). Also, the ZP values tend to be lower in the formulations with higher DOPC composition.

Table 2.1. Composition, physicochemical properties and loading characterization of formulations.

Formulation design	Composition	Particle Size, PS (nm)	Polydispersity Index, PDI (a.u)	Zeta Potential, ZP (mV)	Loading Efficiency, LE (%)	Drug Loading, DL (%)	Drug model
Liposome	DOPC:DPPC 50:50	132 ± 2	0.100	-24.0 ± 4.0	8	40	Sulforhodamine B (SRB)
	DOPC:DPPC 60:40	140 ± 1	0.100	-57.7 ± 1.7	5	27	
	DOPC:DPPC 70:30	133 ± 1	0.070	-60.7 ± 1.6	1	12	
Nanogel	HA + Chitosan	195 ± 0	0.020	+46.3 ± 2.6	96	35	
Microgel*	NIPAM	203 ± 2	0.049	-1.8 ± 0.1	0.7 – N.D.	0.4 - N.D.	Rhodamine 6G (R6G)
	NIPAM-co-MAA 5%	290 ± 4	0.077	-6.3 ± 0.1	1.3 – 3.5	0.8 – 2.1	
	NIPAM-co-MAA 10%	356 ± 4	0.036	-7.0 ± 0.2	10.4 – 38.3	5.9 – 18.7	
	NIPAM-co-MAA 12.5%	496 ± 2	0.123	-7.2 ± 0.3	8.5 – 44.7	4.9 – 21.2	
	NIPAM-co-MAA 15%	501 ± 10	0.121	-8.9 ± 0.1	13.9 – 49.3	7.7 – 22.8	
	NIPAM-co-MAA 20%	512 ± 15	0.080	-10.5 ± 0.4	14.6 – 50.6	8.1 – 23.3	

* Loading efficiencies and drug loading for microgels are given by loading in milliQ water and HEPES 5mM respectively (water –HEPES). Microgel particle size was measured at 26°C, while zeta potential was measured at 22°C.

2.3.2. In vitro release from liposomes

The release profile of sulforhodamine B from the liposomes for the three different formulations that were investigated in 5 mM HEPES and 145 mM NaCl buffer (pH 7.4) at 4°C and 37°C (figure 2.1). As seen in figure 2.1A, the release of sulforhodamine B from all formulations is controlled by two main factors: liposomes composition and the local temperature where the release takes place.

The 50:50 formulation showed significant stability and slow release rate with no burst release at both temperatures due to higher DPPC content in comparison to the other formulations. At 4°C about 41% of liposomes content was released after 72 hours, while 66% was released following 72 hours of incubation at 37°C. The difference in release rates between the two temperatures suggests a significant sensitivity to temperature.

Increase in DOPC concentration in the 60:40 formulation led to an initial burst release and an increase in release rate from liposomes at both temperatures. After 72 hours of release, almost 67% and 78.1% of sulforhodamine B had been released at 4°C and 37°C, respectively. The temperature sensitivity of the 60:40 formulation was noticeably lower than 50:50 formulation (figure 2.1A).

Similarly, sulforhodamine B release behavior presented stronger burst release in the 70:30 formulation compared to that of 60:40 due to higher DOPC content within liposomes structure. Typically, further addition of DOPC in liposomes resulted in depleting about 38% of sulforhodamine B at 4°C and 46% at 37°C within three hours. All loaded sulforhodamine B was released after 24 hours in all cases.

An additional test was performed on the 60:40 formulation by exposing the liposomes to UV light for 15 minutes. The purpose of this test was to identify whether UV light and its thermal energy would affect liposome structural integrity and consequently the sulforhodamine B release rate from liposomes during hydrogel preparations or not. As illustrated in figure 2.1B, sulforhodamine B release was studied by spectrofluorimetry for

1000 seconds (with a registered fluorescence intensity of 15.75 at t= 0 seconds, and 20.33 at t= 1000 seconds). Following 15 minutes of exposure, it had been found that the release rate was moderately changed (68.47 at t=0 seconds, compared to 79.37 at t=1000 seconds). Such increase in the fluorescence intensity of sulforhodamine B can be due to a thermal heating during UV exposure, which could enhance sulforhodamine B release as a result of liposome permeation. Since DOPC represents 60% of the liposomes composition which could altered by higher temperature and affect liposomes structural uniformity. An alternative explanation could be that possible oxidation of the double bonds in DOPC could disrupt the liposomes stability.

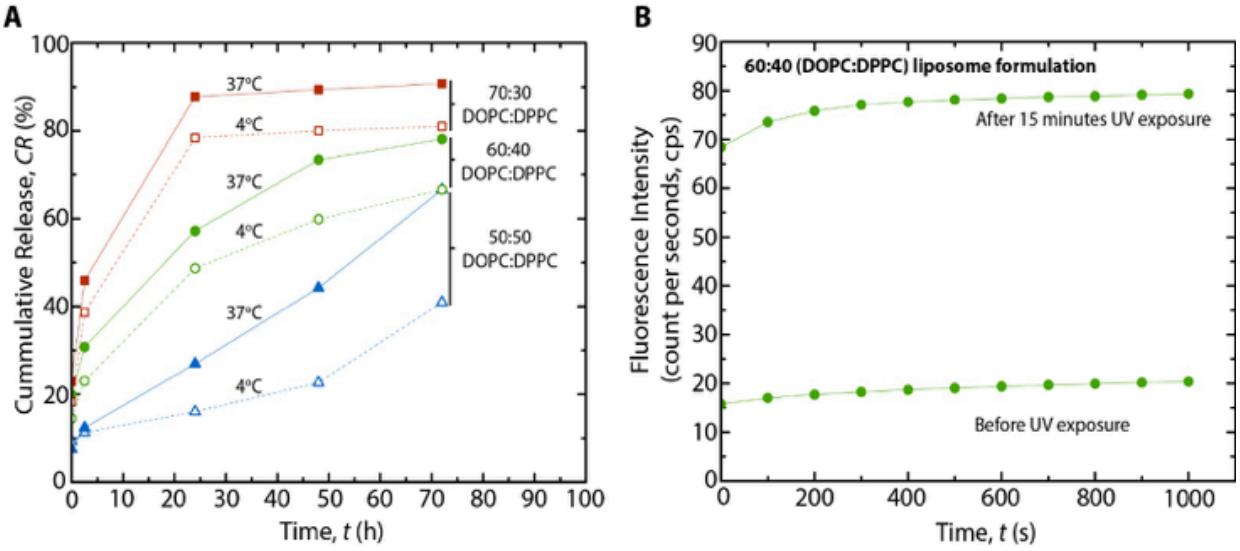

Figure 2.1. Release behaviour of sulforhodamine B from liposomes. (a) Sulforhodamine B release during 72 hours from three different formulations of liposomes at 4 °C and 37 °C. (b) Impact of UV light on sulforhodamine B release during 1000 seconds from (60:40) formulation before and after 15 minutes of exposure.

2.3.3. In vitro release from hydrogel vs. Hydrogel embedding liposomes

The release behaviour of sulforhodamine B from hydrogel only and from liposomes embedded in hydrogels in 5 mM HEPES and 145 mM NaCl buffer (pH 7.4) at 4°C and 37°C for 240 hours is described in figure 2.2.

The free form of sulforhodamine B loaded within the hydrogel without using liposomes has shown very rapid release rate in comparison to liposomes incorporation. Most of the sulforhodamine B content within the hydrogels were released within 24 hours. However, incorporation of liposomes into hydrogels provided a slower and controlled release of sulforhodamine B for all liposome formulations. In the 50:50 formulation, UV light exposure could have been responsible for the initial burst release observed at both temperatures in contrast to the release from liposomes alone before embedding into hydrogels. At 4°C, the cumulative release of sulforhodamine B started at t= 24 hours with 30.37±2.76% of total sulforhodamine B and was slow until t=144 hours when the release increased to a cumulative release of 40.04±2.87%. At t= 240 hours, only 52.36±2.38% of the total quantity of sulforhodamine B loaded within the hydrogel was released. Correspondingly, the 50:50 formulation has shown significant sensitivity to increases in temperature, as revealed by the change of the cumulative release behaviour compared to 4°C. After 24 hours of incubation at 37°C, 49.84±1.03% of sulforhodamine B was diffused from the hydrogel and continued to diffuse until 79.22±4.66% was released after t= 240 hours.

The release behaviour from hydrogels for the 60:40 formulation was also extended until t= 240 hours with superior control compared to liposomes alone. Also, it was observed that significant burst release followed by steady increased release rate every 24 hours at both temperatures. As the DOPC concentration increased in this formulation, the release rate increased slightly in physiological conditions (97.46±3.61% after t= 240 hours) compared to the release at 4°C 86.18±3.24% after t= 240 hours.

The release from hydrogels embedded with the loaded 70:30 formulation was very rapid but still slower than the release of free sulforhodamine B from the hydrogels due to the same factors as in the 60:40 formulation, The hydrogels had released all the free sulforhodamine B after t= 24 hours, while in case of 70:30 the release was completed after t= 48 hours at both 4°C and 37°C.

In order to verify whether intact liposomes have been released from the hydrogels, 10 µL of 1% of octaethylene glycol monododecyl ether (C12E9, purchased from Sigma) detergent were added to the collected supernatants. Results showed an increase in the fluorescence intensity in each sample collected, suggesting that the collected supernatants contained not only free sulforhodamine B, but also liposomes loaded with sulforhodamine B as well (figure 2.2B). Liposomes are released from the hydrogel shortly after incubation was started which suggests that they were located close to hydrogel interface (figure 2.2B). Figure 2.3 depicts this release mechanism.

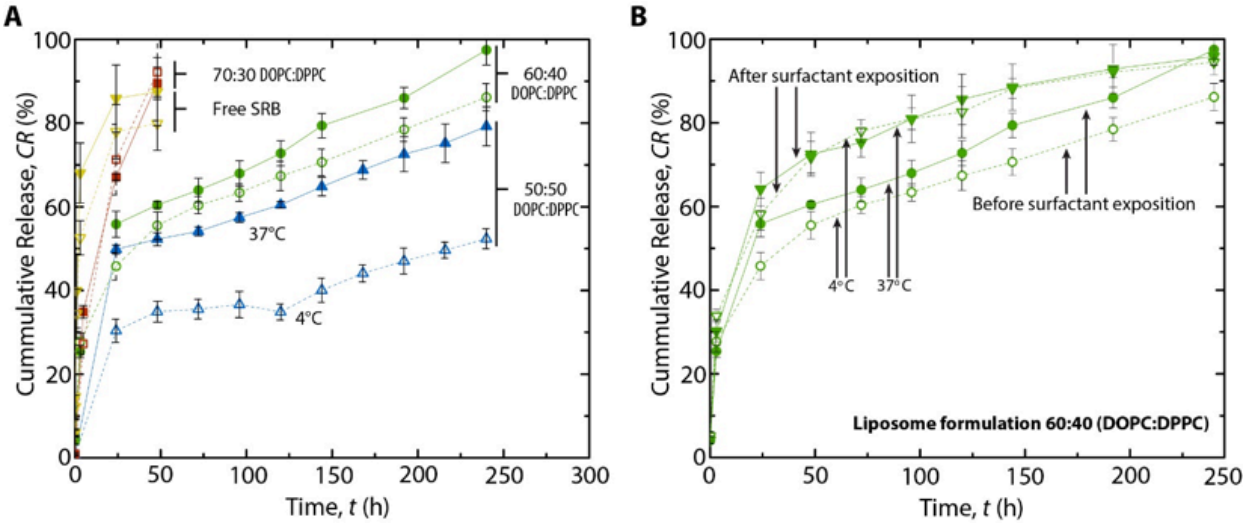

Figure 2.2. Release behavior of sulforhodamine B from hydrogel embedded with liposomes. (a) Sulforhodamine B release after 250 hours from hydrogel embedded with three different formulations of liposomes at 4 °C and 37 °C. (b) An increase in sulforhodamine B release rate from the 60:40 formulation following addition of 1% C12E9 surfactant suggesting liposomes escape from the hydrogel at 4 °C and 37 °C for over 250 hours.

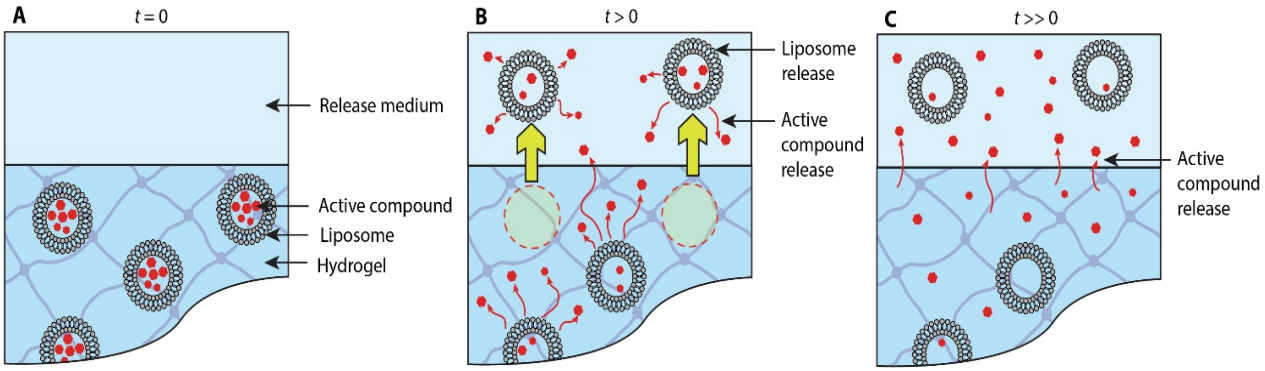

Figure 2.3. Proposed release mechanism of liposomes and sulforhodamine B from hydrogels at different time intervals.

2.3.4. Chitosan nanogels characterization

The chitosan and HA nanogel formulation loaded with surforhodamine B was initially characterized in terms of particle size (42) and zeta potential (ZP) (table 2.1). The particle size showed narrow distribution (PDI = 0.02) and small nanoparticles. The zeta potential indicates a cationic charge (ZP = 46.3 ± 2.6 mV) on the surface of the nanogel and provides insights about its structure. Interestingly, the nanogels seem structured in a way that TPP is interpenetrated within the chains of HA in the core of the nanogel, and chitosan at the periphery of the nanogel, exposing its positive charge.

DL and LE of sulforhodamine B were also evaluated in nanogels by centrifugation. High loading efficiency was achieved (LE= 96%) and consequently achieving high drug loading (DL= 35%) of sulforhodamine B. The chitosan-dense outer shell suggested by ZP data might have facilitated the encapsulation or complexation of surlforhodamine B which carries a net negative charge to the nanogel surface. While keeping its zwitterionic nature at loading pH, it could also have yielded to some interaction with anionic HA or TPP chains, resulting in such high loading.

2.3.5. NIPAM-co-MAA microgels characterization

We have synthesized multiple microgels using NIPAM as a reference structure in which we have added different ratios of MAA, ranging from 5% to 20%. Particle size (42) and ZP were measured separately after purification of the microgel suspensions at 26°C and 22°C respectively (table 2.1). At 26°C, results showed that PS increased with increasing MAA content from 203 nm (MAA 0%) to 512 nm (MAA 20%) and PDI remained below 0.15 for each formulation indicating narrow distribution in milliQ water. ZP decreased with increasing MAA ratios from -6.3 ± 0.1 mV (MAA 5%) up to -10.5 ± 0.4 mV (MAA 20%), while NIPAM without MAA remained mostly neutral (ZP = -1.8 ± 0.1 mV) at 22°C (table 2.1).

Thermo-sensitivity of microgels was also investigated. Particle size was determined from 20°C to 40°C by 2°C increments. The microgels exhibited an increase in collapse temperature by increasing MAA content from 33°C (MAA 0%) to 36°C (MAA 20%) as already reported (43). Collapsed state (T > LCST) was characterized by an approximated 50% PS reduction compared to the swollen state (T < LCST). Interestingly, for MAA ratios higher than 12.5%, a second collapsed state was observed between temperatures 22°C to 26°C (figure S2.1). This observation suggests that MAA distribution in the microgel particle is not homogeneous at such high content leading to richer domains exhibiting different thermal properties. Due to the fact that PS and PDI are similar to those found at low MAA content, it is unlikely that the appearance on this second thermal transition is due to a distinct population of microgel particles formed during the synthesis.

Since all microgels are kept and mostly were used in milliQ water, the effect of the suspension medium on the size of the microgels and on its thermosensitivity was investigated. Compared to milliQ water, microgels in saline solution (Phosphate 10mM + 145 mM NaCl) without MAA started to aggregate at 32°C (figure S2.1) where it usually starts to collapse (T > LCST). In this case the salt is the major cause of aggregation since, as reported by many studies, the salt reduced electrostatic repulsion of each particles causing them to aggregate. Interestingly, such aggregation was not observed with NIPAM-co-MAA microgels, suggesting that the 5% MAA content was sufficient to keep colloidal stability in simulated physiological

conditions. However, a reduced thermosensitivity of microgels was observed in PBS (table 2.2). The increased pH compared to milliQ water might have increased carboxylic acid group ionisation, and in addition with the presence of salt, increased water content and its hydrophilic property opposing from the collapse usually observed at 32°C - 34°C. This effect was even more pronounced in HEPES 5 mM. Microgels containing 20% MAA did not even present a clear distinction between the collapsed nor the swollen state. However, this microgel increased so much in terms of size that was near reliable limit of the DLS device detection / quantification. Since this phenomenon for most microgels was observed, it can be explained that without salt but at pH 7.4, electrostatic repulsions within the microgel are so effective that it is nearly preventing the microgel to collapse above the LCST of NIPAM. As a result, the size variation of microgels (collapsed vs. swelled) in HEPES was caused by reduction in NIPAM-co-MAA polymers thermo-sensitivity as seen in fig.S2.1. This hypothesis is also supported by the size variation of NIPAM without MAA in HEPES, which exhibited collapse similar as in water before its aggregation. The NIPAM aggregation in buffered medium (pH = 7.4) without salt indicates that the ionic force from HEPES 5 mM was sufficient to initiate the aggregation, which is an insight of a very weak colloidal stability. However, this microgel might not be very suitable for physiological applications while the addition of MAA in NIPAM structure eliminates this concern.

Additionally, the surface charge of microgels was also influenced by temperature. It was observed that increasing the temperature decreased the ZP of the microgels. This behavior can be explained considering that upon collapsing the sulfated end chains from the initiator as well as MAA are expelled from the core of the microgel thus increasing ZP. This mechanism also supports the results observed with NIPAM without MAA, which demonstrated increase in ZP from a quasi-neutral charge (-1.8 mV) at 22°C to a more polarized surface (-11.8 mV) at 38°C. Such ZP decrease was also observed with the other microgels, but to a lower extent. For the release studies, microgels were loaded with R6G using the standard loading procedure described in the methodology section. DL and LE were determined in milliQ water medium and in HEPES 5 mM without salt and were expressed in percentage (table 2.1). Particles with no MAA incubated in water and HEPES without salt and particles with 5% MAA incubated in water were not tested for release studies in hydrogels since they demonstrated very low DL

and LE. Although, very high DL (23.3%) and LE (50.6%) were achieved in HEPES without salt after purification using MAA 20% microgels, hence reducing the total particle amount needed for reaching 0.27 mg R6G in the hydrogels for release purposes.

2.3.5.1. NIPAM-co-MAA microgels DL and LE characterization

To gain more insights into the parameters that influence the microgel's capabilities to encapsulate R6G, a complete evaluation of DL and LE as a function of MAA ratio, R6G / particle ratio, incubation medium and incubation temperature was performed (see figure 2.4).

At first, microgels were incubated with R6G at different concentration for 1 hour at 25°C in pure water. DL was determined for each ratios of MAA in microgels represented in figure 2.4A. Noticeably, NIPAM without MAA did not demonstrate significant encapsulation of R6G at any R6G ratios in pure water. However, the presence of MAA in the microgel structure significantly increased DL and LE from 0% for microgels containing no MAA up to 16.3% (DL) and 32.4% (LE) for 20% MAA, for instance, at a R6G/Particle ratio of 0.6. As can be seen in figure 2.4A, 2.4B, and in table 2.1, by increasing the MAA content in the microgel, the DL and LE increased as well. The effect of MAA concentration in microgels on DL and LE was also found (quite well) correlated with the effect of MAA on ZP. Likewise, increasing the drug per particle ratio increased DL up to a ratio of 0.6 then decreased afterward, meaning that maximum loading reached at this ratio. Above 0.6 ratio, LE decreased as well, as shown in figure 2.4B, indicating that there was an increasingly higher concentration of free R6G remaining after loading, thus increasing the need for extensive purification.

We found that these results were finely correlated with the Langmuir isotherms equations. As it was suggested by Grosberg *et al.* (44), it was possible to determine the affinity and the quantity bound to macroscopic hydrogels by adsorption. More recently, this equation was applied to microgels and was shown as a promising tool for drug-microgels interactions models. The Langmuir adsorption isotherm equation is given below:

$$D_{ad} = \frac{S \times K \times D_{sol}}{K \times D_{sol} + 1} \quad \text{(Eq. 2.3)}$$

D_{ad} is the concentration (mmol/L) of R6G adsorbed on the microgel, D_{sol} is the concentration (mmol/L) of free R6G remaining in solution, S is the concentration (mmol/L) of maximum adsorption and K is the affinity constant of R6G to its adsorption site (L/mmol). Using Origin Pro 8.5® we fitted the equations on R6G adsorbed concentration in function of free R6G concentration in order to determine S and K (figure 2.5A). Since K should be the same for each microgels with content in MAA>0% (adsorption site) K was kept constant.

The overall affinity, Q, of R6G to the microgels was calculated by multiplying S and K, resulting in unitless value. This value was plotted in function of MAA content in microgels (figure 2.5B). The result is the expression of a quasi-proportional linear regression supported by Adj-R^2 higher than 0.95. The slope indicates that using NIPAM microgels containing higher percentage of MAA is directly proportional to microgels affinity to R6G. However, as it was observed with the size thermo-sensitivity assay, the appearance of nano-domains richer in MAA could alter this correlation at higher MAA content in the microgels with more important structure changes. These results also supports that the R6G is mostly adsorbed to the microgels by electrostatic interaction since its affinity is linearly proportional to the concentration of MAA in the microgel if the structures remain similar and loading mediums are identical.

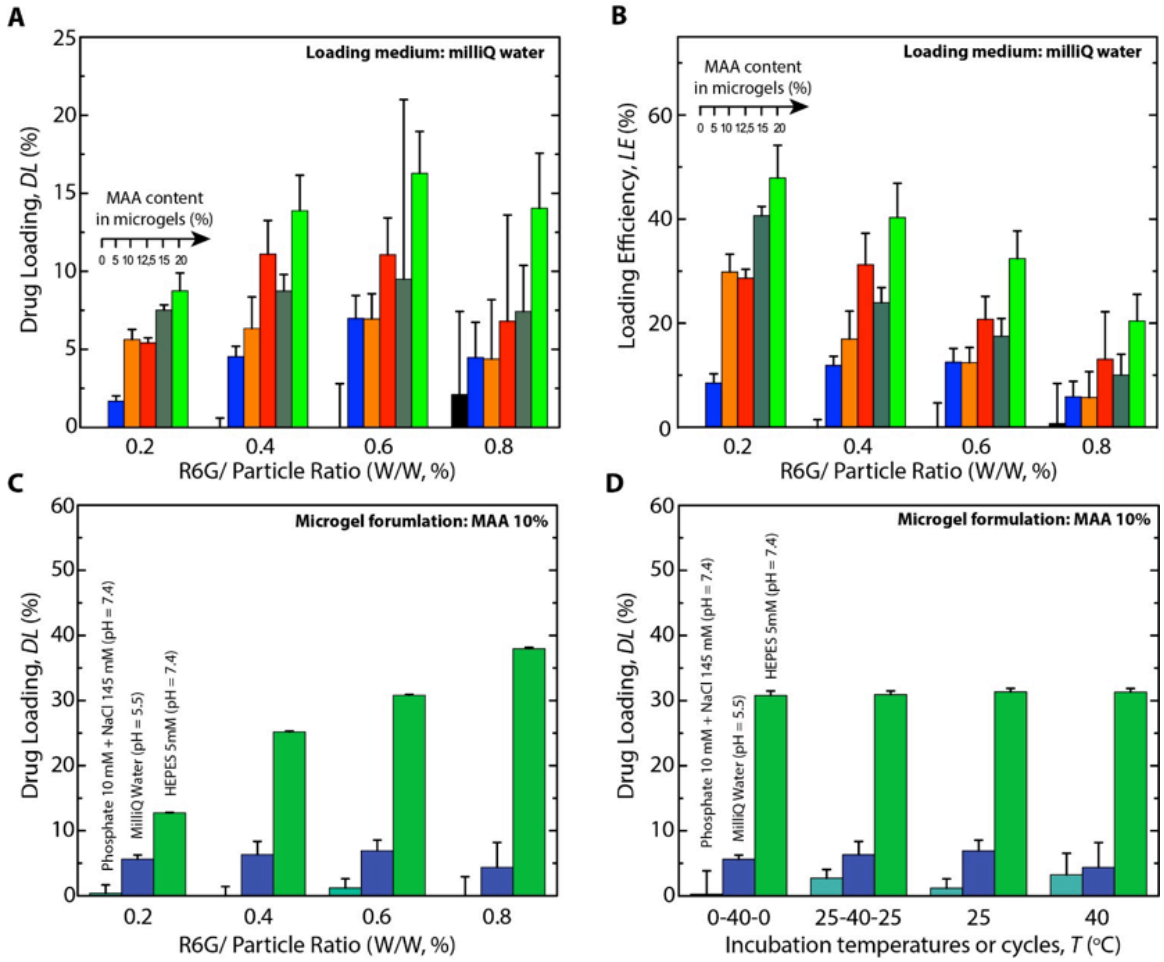

Figure 2.4. Characterization of R6G loading in NIPAM-co-MAA microgels. Microgels containing 0 to 20% MAA were loaded with R6G in pure water and (a) drug loading and (b) loading efficiency were determined at different R6G / particle ratio. Drug loading for MAA 10% microgels were determined in PBS 10 mM with 145 mM NaCl (pH = 7.4), pure water and in HEPES 5mM without salt (pH = 7.4) at (c) different R6G / particle ratio and at (d) different static temperatures and temperature cycles. If not mentioned, incubation temperature was set to 25°C for one hour.

Different temperatures and different incubation media were also evaluated in terms of DL using one microgel formulation (MAA 10%) as illustrated in figure 2.4C and 2.4D. In HEPES 5 mM (pH = 7.4) we observed a high level of loaded R6G (38%) compared to pure water (pH = 5.5). We hypothesized that this increase is mostly due to effect of pH being higher in HEPES, increasing ionization of COOH groups and therefore increasing electrostatic interaction between R6G and the COO^- present in the microgel. This is supported by reported

values of pKa of the microgels containing MAA between 5 and 6 (45). Consequently, switching from a medium at pH = 5.5 to pH = 7.4 would lead to an increase in ionization of the COOH groups in the microgels. No peak or plateau was reached in terms of DL in HEPES 5 mM at ratios from 0.2 to 0.8, meaning, achieving higher DL with R6G/particle ratio higher than 0.8 should be possible. The addition of salt further confirmed the fact that electrostatic interactions are the primary interactions responsible for drug loading. DL in PBS 10 mM and NaCl 145 mM at pH = 7.4 was close to 0% and compared to both media previously described was significantly reduced for every R6G/Particle ratio used, the latter having no effect on DL in buffered saline.

Additionally, the affinity *Q*, of R6G on microgels using all three different incubation media was determined using *K* and *S* parameters from Langmuir isotherm as described previously. Resulting affinity *Q* was compared with all three media used for loading (figure 2.5C). The calculated affinity for milliQ water (pH = 5.5) was evaluated at 1.1 ± 0.3, phosphate 10 mM with NaCl 145 mM at 0.04 ± 0.04 and HEPES 5 mM at 6.4 ± 0.5. Without presence of ions and at slightly acidic pH affinity was almost 6-fold lower compared to a pH of 7.4 with the presence of very few ions, supporting an ionization of the COOH groups in the microgel. However, by increasing the concentration of counter-ions such as NaCl, the affinity for microgel decreases drastically.

The thermo-sensitivity of microgels was tested to investigate the potential for increasing the drug loading capabilities by successive swelling and collapsing cycles (39, 46). This process had the potential to maximize the penetration of R6G within the core of the particle thus increasing DL. Using three different incubation media (pure water, HEPES 5 mM and PBS 10 mM + NaCl 145 mM), incubation temperatures of 25°C and 40°C and incubation temperature cycles of 0-40-0°C and 25-40-25°C, no significant differences on DL were found for each temperature, as illustrated in figure 2.4D. This result suggests that the inner and outer parts of the microgel quickly equilibrate. The Langmuir isotherm was not applied since no variation of DL was observed for all temperatures assayed. The Langmuir isotherm was not applied since no variation of DL was observed for all temperatures assayed.

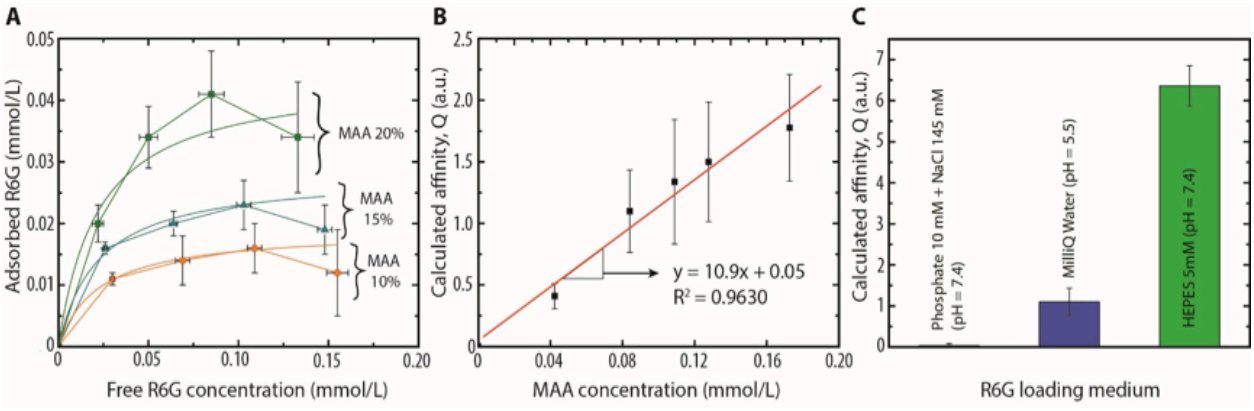

Figure 2.5. Characterization of R6G affinity to microgels. Langmuir isotherms for microgels (A) for 3 microgels, where the affinity *Q* was determined and plotted in function of MAA concentration (B). The affinity for R6G to microgels are also presented in three mediums and conditions (C).

2.3.6. In vitro release from hydrogel embedding microgels or nanogels

The release kinetic of NIPAM-co-MAA microgels and chitosan-HA nanogels embedded in AAm/BisAc hydrogel was followed over 72 hours at 4°C and 37°C as presented in figure 2.6. The drug release studies were all performed in a HEPES buffer (HEPES 5 mM + NaCl 145 mM).

The release curves of the different embedded microgels can be explained by two different release behaviours (figure 2.6A). The initial release shows a constant first-order release kinetic suggesting an affinity-based release. Thereafter, a much slower release rate is observed after a 60-70% cumulative release of R6G. This “break point” was calculated by drawing the release linear curves for both release kinetics on OriginPro 8.5®. The “break point” was determined where both release curves cross for each microgels formulations in table 2.2.

Loaded in HEPES 5mM, the tested microgel formulations initially released 58-82% of the R6Gs within 5 to 25 hours at 37°C, until reaching the “break-point”, as shown in table 2.2. The release kinetics of R6G from microgels loaded in pure water were also evaluated in

HEPES buffer for 72 hours (figure 2.6B). Each tested formulation demonstrated similar initial release profiles with 64-71% released in 4 to 8 hours (table 2.2). Hydrogels containing free R6G initially released slightly faster in comparison to hydrogels embedded with microgels, which release their contents over 4-8 hours (63-66%) in comparison. Despite a fast release at 37°C, hydrogels embedded with microgels loaded in HEPES show the potential to sustain release up to 10.7 hours compared to hydrogels containing free R6G since the "break point" was reached after only 4 hours. Similarly, embedded microgels loaded in pure water also reached the "break point" at 8.3 hours. The results suggest that the R6G loading medium did not impact the R6G release rate nor its release mechanism. Additionally no clear correlation between release rate and the MAA ratio in microgels was observed. However, the presence of microgels could be responsible for the reduced release rate.

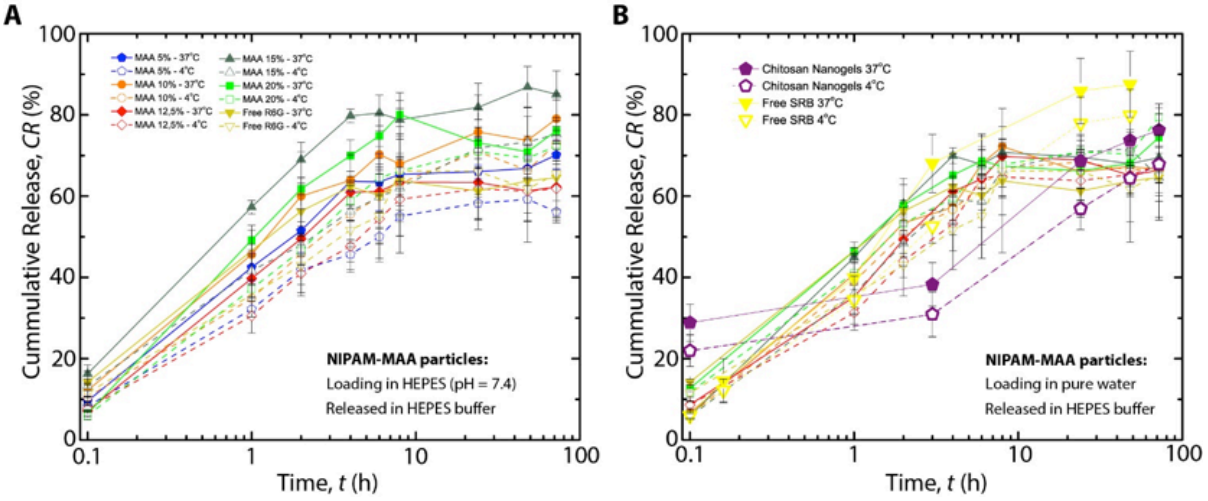

Figure 2.6. Release kinetics of microgel and nanogel formulations embedded in hydrogel structures at 4°C and 37°C. (a) Release kinetics of R6G were followed for 72 hours for each microgel formulations loaded with R6G in HEPES 5 mM without salt and (b) in pure water. Release of sulforhodamine B from nanogels was also studied along with microgels initially loaded in water.

For the purpose of studying temperature effects and release mechanism on drug release, R6G release was also evaluated at 4°C for 72 hours (figure 2.6B). It was found that R6G initially released (loaded in HEPES 5 mM) 58- 72% for each microgel after approximately 11 - 25 hours (table 2.2). Comparatively, the microgels loaded in pure water released 64-69% of its total contents in 7-9 hours and free R6G released 65.8% within 7.6 hours until the "break point". Release results at 4°C also support the hypothesis that increased sustained release using microgels allow for an extra 3-17 hours of release (microgels loaded in HEPES for instance) compared to free R6G. Likewise, temperature increased the rate at which the "break point" was reached at 4°C compared to 37°C. This effect is independent of the R6G initially loading medium (Figure 2.6A and 2.6B). This can be explained by the reduced solubility of R6G in buffered saline at 4°C, decreasing its mobility through the hydrogel network. In addition, the thermo-sensitivity of microgels might have influenced the release rates. Since the hydrogel is polymerized at room temperature the microgels are swollen, but at release temperature of 37°C, it shrinks, expelling R6G from its shell and leaving a *"*micropore*"* network within the hydrogel, thus facilitating R6G release. In comparison, this phenomenon would not occur at 4°C since microgels would remain in a swelled state.

Release from chitosan and HA nanogels was performed by the same method. The incubation at both 4°C and 37°C, cumulative release (CR) of sulforhodamine B was evaluated over 72 hours. The resulting release kinetics represented in figure 2.6B was compared with hydrogels containing free sulforhodamine B (figure 2.6B). Chitosan nanogels released sulforhodamine B in a more controlled fashion than its free form. Nanogels embedded in hydrogels released 73.7±2.0% over a period of 48 hours at 37°C and 64.4±3.8% in the same timeframe at 4°C, while 85.8±7.1% and 77.9±6.4% of free sulforhodamine B were released from hydrogel at 37°C and 4°C respectively within 24 hours. Although a high burst effect (21-29%) can be observed initially from embedded nanogels, suggesting an immediate release of sulforhodamine B upon swelling in the incubation medium. Conversely, lowering temperature decreased the release rate by reducing the CR by 9% at 4°C in nanogel systems embedded in hydrogel. The results suggest that embedding nanogel significantly impacted the release profiles of the sulforhodamine B from the hydrogels by altering its release pattern in more controlled fashion.

Table 2.2. Release curve "break points" for affinity-based systems (microgels and free R6G or SRB)

Particle	Loading medium	Incubation temperature = 37°C		Incubation temperature = 4°C	
		Release time (h)	% Released	Release time (h)	% Released
MAA5%	HEPES 5 mM	5.0 h	65.1	11.0 h	57.7
	Water	N.D	N.D	N.D	N.D
MAA10%	HEPES 5 mM	10.7 h	74.8	22.7 h	72.6
	Water	7.6 h	71.0	8.2 h	66.3
MAA12.5%	HEPES 5 mM	5.5 h	62.5	11.6 h	60.9
	Water	8.3 h	69.0	7.0 h	64.3
MAA15%	HEPES 5 mM	4.9 h	81.6	25.2 h	72.4
	Water	4.3 h	70.0	9.2 h	68.0
MAA 20%	HEPES 5 mM	7.2 h	78.7	13.0 h	70.2
	Water	6.0 h	68.6	8.9 h	69.3
Free R6G	N/A	4.0 h	62.5	7.6 h	65.8
Free SRB	N/A	3.9 h	73.6	21.2 h	77.6

2.3.7. Release profiles from hydrogels embedding liposomes and microgels

The inclusion of three different formulations of nanocarriers within hydrogels and their different release profiles are multiples factors related. Liposomes usually are a layer or bi-layer of phospholipids with different compositon where they can entrap hydrosoluble drugs within their hollowed structure. Nanogels and microgels are made from hydrophilic polymers swelled in water and can also encapsulate / adsorb drugs. Differences in the encapsulation or adsorption properties of nanoparticles lead to major differences in the release kinetics from hydrogels. Since the liposomes consist mainly of lipids, the release kinetics from liposomes embedded in hydrogel could be estimated by the diffusion coefficient of the drug within the liposome bi-layer. Similarly, the release profiles from microgel embedded in hydrogel could be also estimated by the affinity of the drug to the microgel. Equation modeling these different profiles has been described in recent studies (Eq. 2.4) (47).

$$t^* = \frac{t}{\frac{L^2}{D} \times (1 + K \times C_{NP})} \qquad \text{(Eq. 2.4)}$$

t^* is the adjusted time (adimensional), t is the time (h), L^2 is the thickness of the hydrogel (48), D is the diffusion coefficient (cm^2/s), K is the affinity constant of the (mM^{-1}) drug with the particle and C_{NP} as the concentration of particles / binding site (mM).

(Eq. 2.4) was discussed in a study in order to collapse different release profiles from nanoparticles embedded within hydrogels into single master curve based on the parameters that affect the release rate. These parameters include the diffusion factor ($\frac{\boldsymbol{L^2}}{\boldsymbol{D}}$) from Fick's second law of diffusion and affinity factor ($\boldsymbol{1 + K \times C_{NP}}$) from Langmuir isotherm eqation.

We assumed that the affinity of sulforhodamine B to the liposomes does not vary significantly with changing phospholipids composition (50:50, 60:40, 70:30). Since sulforhodamine B is hydrophilic, most of the sulforhodamine B will be encapsulated within the liposome cavity rather than being bound to the lipid bilayer, hence the affinity should be <<1. The time was adjusted using the following simplified equation (Eq. 2.5):

$$t^* = \frac{t \times D}{L^2} \qquad \text{(Eq. 2.5)}$$

The diffusion coefficient of the liposomes embedded in hydrogel was determined by calculating the effective diffusion coefficient (D_{eff}) using Fick's second law, where the diffusion in solid may be expressed as in (Eq. 2.6) (49):

$$CR\% = 2 \times \left(\frac{D_{eff} \times t}{\pi \times L^2}\right)^{1/2} \qquad \text{(Eq. 2.6)}$$

CR% corresponds to the cumulative release of the drug, t is the time (hour), L^2 is the thickness of the hydrogels cylinders (5 mm). The release kinetics were fitted using this equation and D_{eff} was obtained for each liposome formulations.

The application of the equation using the collected D_{eff} (table 2.3) yielded a collapse in the release curves of liposomes with all different compositions embedded in hydrogels (figure 2.7A). This collapse suggests that the observed release kinetics were mostly controlled by the coefficient of diffusion, also expressed by the square root release kinetic observed in figure 2.7A. It was expected that release curves from diffusion-based controlled systems would collapse into one curve by adjusting the time through normalizing diffusion coefficient in Eq. 2.4. Release curves remained collapsed which supports the assumption that *K* does not vary significantly with changing phospholipids composition. Thus, diffusion is the major mechanism through which the sulforhodamine B is released.

In contrast, microgels are most likely to follow an affinity based release profile. Microgels embedded in hydrogel release curves were then adjusted using the following simplified equation from Eq. 2.4:

$$t^* = \frac{t}{(1+K\times C_{MAA})} \qquad \text{(Eq. 2.7)}$$

Since *K* was already calculated from Langmuir isotherms, they were directly integrated in the equation and time was adjusted with according parameters. We omitted the diffusion factor of Eq.2.4 ($\frac{L^2}{D}$), since it is the same for every microgel formulation.

Resulting curves were quite similar as it initially was, but show better superposition range (figure 2.7B). Such results confirm that the presence of the microgel does affect the release kinetic but is mostly affected by the affinity of the R6G-microgel. Additionally, the differences between the slope at 37°C and 4°C is more important, confirming the small temperature effect. The slope variation might be the result of a diminished diffusion coefficient in the R6G due to a reduced mobility at 4°C.

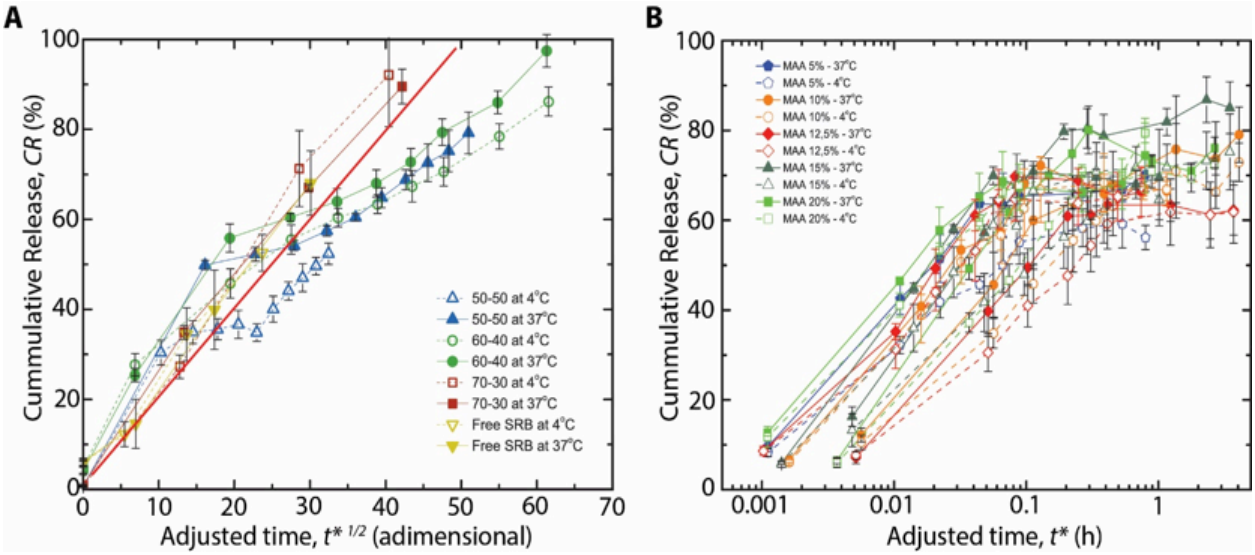

Figure 2.7. Release curves time adjustment of liposomes and microgels embedded in hydrogels. Adjustment of time in function of hydrogel thickness and diffusion coefficient (Eq. 2.5) on liposomes (A) and adjustment based on R6G affinity with the microgel loaded from both water and HEPES 5mM (B). In comparison with their respective unadjusted release curves, an effect of superposition should be created with both adjustments.

Table 2.3. Diffusion and affinity key parameters for R6G and sulforhodamine B release.

Formulation design	Composition	D_{eff} (cm^2/h)	K $(mmol/L)^{-1}$
Liposome	**DOPC:DPPC 50:50**	**2.7**	**-**
	DOPC:DPPC 60:40	**3.9**	**-**
	DOPC:DPPC 70:30	**8.5**	**-**
Nanogel	**HA + Chitosan**	**30.8**	**0.16**
Microgel	**NIPAM**	**-**	**-**
	NIPAM-co-MAA 5%	**75.5**	**45**
	NIPAM-co-MAA 10%	**75.5**	**45**
	NIPAM-co-MAA 12.5%	**75.5**	**45**
	NIPAM-co-MAA 15%	**75.5**	**45**
	NIPAM-co-MAA 20%	**75.5**	**45**

To summarize, it has been demonstrated that NIPAM-co-MAA microgels have the capability to prolong the time of release. More considerably, chitosan-HA nanogels have the capacity for a finer control than microgels by one extra day but were not as sensitive to temperature. However, use of microgels or nanogels does not sufficiently control the release of their active compound to produce the zero-order release kinetic, which is possible with liposomes.

2.4. Conclusion

The research goal was to determine a method to produce highly stable liposomes, microgels, and nanogels embedded in hydrogels by modifying their compositions and concentrations to ensure controlled release of active compounds. We demonstrated the main release mechanism of each system and provided methods to better predict and understand the key parameters involved in drug-loading and controlled release systems, and how they influence the release from a model hydrogel matrix containing nano-inclusions. Affinity-based

nano-inclusions yielded a better drug-loading tuning within the hydrogel but did not sustain the rate of active compound release compared to liposomal systems. For the liposome based system, it was found that it is easier to adjust the release rate by simply altering lipid composition and diffusivity of the active compond. The results also have showed that embedding nanocarriers within hydrogels has helped to improve the loaded nanocarriers stability and to control the release over time.

2.5. References

1. Wang AZ, Gu F, Zhang L, Chan JM, Radovic-Moreno A, Shaikh MR, et al. Biofunctionalized targeted nanoparticles for therapeutic applications. 2008.

2. Plamper FA, Ruppel M, Schmalz A, Borisov O, Ballauff M, Müller AH. Tuning the thermoresponsive properties of weak polyelectrolytes: aqueous solutions of star-shaped and linear poly (N, N-dimethylaminoethyl methacrylate). Macromolecules. 2007;40(23):8361-6.

3. Wei J, Chen F, Shin J-W, Hong H, Dai C, Su J, et al. Preparation and characterization of bioactive mesoporous wollastonite–polycaprolactone composite scaffold. Biomaterials. 2009;30(6):1080-8.

4. Smith A. Evaluation of poly (lactic acid) as a biodegradable drug delivery system for parenteral administration. International journal of pharmaceutics. 1986;30(2):215-20.

5. Bala I, Hariharan S, Kumar MR. PLGA nanoparticles in drug delivery: the state of the art. Critical Reviews™ in Therapeutic Drug Carrier Systems. 2004;21(5).

6. Nair M, Tan JS. Microgel drug delivery system. Google Patents; 1992.

7. Richardson TP, Peters MC, Ennett AB, Mooney DJ. Polymeric system for dual growth factor delivery. Nature biotechnology. 2001;19(11):1029-34.

8. Lehár J, Krueger AS, Avery W, Heilbut AM, Johansen LM, Price ER, et al. Synergistic drug combinations tend to improve therapeutically relevant selectivity. Nature biotechnology. 2009;27(7):659-66.

9. Hennink W, Van Nostrum CF. Novel crosslinking methods to design hydrogels. Advanced drug delivery reviews. 2012;64:223-36.

10. Xiang T-X, Anderson BD. Liposomal drug transport: a molecular perspective from molecular dynamics simulations in lipid bilayers. Advanced drug delivery reviews. 2006;58(12):1357-78.

11. Torchilin VP. Recent advances with liposomes as pharmaceutical carriers. Nat Rev Drug Discov. 2005;4(2):145-60.

12. Laouini A, Jaafar-Maalej C, Limayem-Blouza I, Sfar S, Charcosset C, Fessi H. Preparation, Characterization and Applications of Liposomes: State of the Art. Journal of Colloid Science and Biotechnology. 2012;1(2):147-68.

13. Raemdonck K, Demeester J, De Smedt S. Advanced nanogel engineering for drug delivery. Soft Matter. 2009;5(4):707-15.
14. Malmsten M. Soft drug delivery systems. Soft Matter. 2006;2(9):760-9.
15. Sonia TA, Sharma C. Chitosan and Its Derivatives for Drug Delivery Perspective. In: Jayakumar R, Prabaharan M, Muzzarelli RAA, editors. Chitosan for Biomaterials I. Advances in Polymer Science. 243: Springer Berlin Heidelberg; 2011. p. 23-53.
16. Berth G, Dautzenberg H. The degree of acetylation of chitosans and its effect on the chain conformation in aqueous solution. Carbohydrate Polymers. 2002;47(1):39-51.
17. Anthonsen MW, Vårum KM, Smidsrød O. Solution properties of chitosans: conformation and chain stiffness of chitosans with different degrees of N-acetylation. Carbohydrate Polymers. 1993;22(3):193-201.
18. Schatz C, Viton C, Delair T, Pichot C, Domard A. Typical Physicochemical Behaviors of Chitosan in Aqueous Solution. Biomacromolecules. 2003;4(3):641-8.
19. Sorlier P, Denuzière A, Viton C, Domard A. Relation between the Degree of Acetylation and the Electrostatic Properties of Chitin and Chitosan. Biomacromolecules. 2001;2(3):765-72.
20. Sorlier P, Rochas C, Morfin I, Viton C, Domard A. Light Scattering Studies of the Solution Properties of Chitosans of Varying Degrees of Acetylation. Biomacromolecules. 2003;4(4):1034-40.
21. Francis Suh JK, Matthew HWT. Application of chitosan-based polysaccharide biomaterials in cartilage tissue engineering: a review. Biomaterials. 2000;21(24):2589-98.
22. Agnihotri SA, Mallikarjuna NN, Aminabhavi TM. Recent advances on chitosan-based micro- and nanoparticles in drug delivery. Journal of Controlled Release. 2004;100(1):5-28.
23. Mura S, Nicolas J, Couvreur P. Stimuli-responsive nanocarriers for drug delivery. Nat Mater. 2013;12(11):991-1003.
24. Bartlett RL, Panitch A. Thermosensitive Nanoparticles with pH-Triggered Degradation and Release of Anti-inflammatory Cell-Penetrating Peptides. Biomacromolecules. 2012;13(8):2578-84.
25. Yang X, Lee HY, Kim J-C. pH- and Temperature-sensitive Nanoparticles Prepared using Salt Bridge. Journal of Macromolecular Science, Part A. 2009;46(10):959-66.

26. Pelton RH, Chibante P. Preparation of aqueous latices with N-isopropylacrylamide. Colloids and Surfaces. 1986;20(3):247-56.
27. Guan Y, Zhang Y. PNIPAM microgels for biomedical applications: from dispersed particles to 3D assemblies. Soft Matter. 2011;7(14):6375-84.
28. Hu X, Tong Z, Lyon LA. Control of poly(N-isopropylacrylamide) microgel network structure by precipitation polymerization near the lower critical solution temperature. Langmuir. 2011;27(7):4142-8.
29. Saikia AK, Aggarwal S, Mandal UK. Preparation and Controlled Drug Release Characteristics of Thermoresponsive PEG/Poly (NIPAM-co-AMPS) Hydrogels. International Journal of Polymeric Materials and Polymeric Biomaterials. 2012;62(1):39-44.
30. Hoare T, Pelton R. Impact of Microgel Morphology on Functionalized Microgel−Drug Interactions. Langmuir. 2008;24(3):1005-12.
31. Hanauer N, Latreille PL, Alsharif S, Banquy X. 2D, 3D and 4D active compound delivery in tissue engineering and regenerative medicine. Curr Pharm Des. 2015;21(12):1506-16.
32. Goldberg M, Langer R, Jia X. Nanostructured materials for applications in drug delivery and tissue engineering. Journal of biomaterials science Polymer edition. 2007;18(3):241-68.
33. Numata K, Yamazaki S, Naga N. Biocompatible and biodegradable dual-drug release system based on silk hydrogel containing silk nanoparticles. Biomacromolecules. 2012;13(5):1383-9.
34. Gao W, Vecchio D, Li J, Zhu J, Zhang Q, Fu V, et al. Hydrogel containing nanoparticle-stabilized liposomes for topical antimicrobial delivery. ACS nano. 2014;8(3):2900-7.
35. Glotzer SC, Solomon MJ. Anisotropy of building blocks and their assembly into complex structures. Nature materials. 2007;6(8):557-62.
36. Gan Q, Wang T, Cochrane C, McCarron P. Modulation of surface charge, particle size and morphological properties of chitosan–TPP nanoparticles intended for gene delivery. Colloids and Surfaces B: Biointerfaces. 2005;44(2–3):65-73.
37. López-León T, Ortega-Vinuesa JL, Bastos-González D, Elaïssari A. Cationic and Anionic Poly(N-isopropylacrylamide) Based Submicron Gel Particles: Electrokinetic Properties and Colloidal Stability. The Journal of Physical Chemistry B. 2006;110(10):4629-36.
38. Ku B, Seo H, Chung B. Synthesis and characterization of thermoresponsive polymeric nanoparticles. BioChip J. 2014;8(1):8-14.

39. Kleinen J, Klee A, Richtering W. Influence of architecture on the interaction of negatively charged multisensitive poly(N-isopropylacrylamide)-co-methacrylic acid microgels with oppositely charged polyelectrolyte: absorption vs adsorption. Langmuir. 2010;26(13):11258-65.
40. Baier Leach J, Bivens KA, Patrick Jr CW, Schmidt CE. Photocrosslinked hyaluronic acid hydrogels: Natural, biodegradable tissue engineering scaffolds. Biotechnology and Bioengineering. 2003;82(5):578-89.
41. Barenholz, Y. and Amselem, S.. Liposome Technology. 1993, 2nd edition, Vol. I, p. 527, CRC Press, Boca Raton, FL.
42. Barenholz Y, Gibbes D, Litman B, Goll J, Thompson T, Carlson F. A simple method for the preparation of homogeneous phospholipid vesicles. Biochemistry. 1977;16(12):2806-10.
43. Hoare T, Pelton R. Functionalized Microgel Swelling: Comparing Theory and Experiment. The Journal of Physical Chemistry B. 2007;111(41):11895-906.
44. Ito K, Chuang J, Alvarez-Lorenzo C, Watanabe T, Ando N, Grosberg AY. Multiple point adsorption in a heteropolymer gel and the Tanaka approach to imprinting: experiment and theory. Progress in Polymer Science. 2003;28(10):1489-515.
45. Dong H, Du H, Qian X. Theoretical Prediction of pKa Values for Methacrylic Acid Oligomers Using Combined Quantum Mechanical and Continuum Solvation Methods. The Journal of Physical Chemistry A. 2008;112(49):12687-94.
46. Kabanov AV, Vinogradov SV. Nanogels as Pharmaceutical Carriers: Finite Networks of Infinite Capabilities. Angewandte Chemie (International ed in English). 2009;48(30):5418-29.
47. Vulic K, Pakulska MM, Sonthalia R, Ramachandran A, Shoichet MS. Mathematical model accurately predicts protein release from an affinity-based delivery system. Journal of Controlled Release. 2015;197:69-77.
48. Tyrrell D, Heath T, Colley C, Ryman BE. New aspects of liposomes. Biochimica et Biophysica Acta (BBA)-Reviews on Biomembranes. 1976;457(3):259-302.
49. Pjanović R, Bošković-Vragolović N, Veljković-Giga J, Garić-Grulović R, Pejanović S, Bugarski B. Diffusion of drugs from hydrogels and liposomes as drug carriers. Journal of Chemical Technology & Biotechnology. 2010;85(5):693-8.

Chapter 3 : Discussion

3.1. Discussion

In this study, our objective was to develop an enhanced controlled delivery system based on embedding different nanocarriers (liposomes, nanogels, microgels) loaded with model active compounds within hydrogels. A structured hydrogel was created with embedded nanocarriers separately loaded with model active compounds that would be released in a controlled fashion by manipulating different parameters of temperature and nanocarriers' composition and concentration.

We compared drug loading and release kinetics of sulforhodamine B using liposomes composed of DOPC and DPPC at different ratios, nanogels of CS/HA, and the release kinetics of rhodamine 6G using NIPAM microgels with different ratios of MAA embedded in a model hydrogel of acrylamide.

Performing the release study from liposomes alone or embedded in hydrogels at 4°C has helped to maintain and decrease the release rate of sulforhodamine B significantly compared to 37°C in the (50:50) formulation but less efficiently in (60:40) and (70:30) formulations (figure 2.1A and figure 2.2A). The difference in release rate between the 50:50 formulation at various temperatures suggests a significant influence towards temperature. This can be explained by DOPC phospholipid having very low transition temperature (-22°C) comparing to release conditions and at 37°C it is relatively close to transition temperature of DPPC phospholipid (41°C) which lead to liposomes permeation. Temperature has greater influence over formulations of (60:40) and (70:30) due to presence two different components of phospholipids with higher component of DOPC (1, 2). Liposome stability is directly related to lipid acyl chain type, which is consequently related to variability of phase transition temperatures (3). As a result, the liposomal phospholipids membrane barrier efficacy will significantly change near phase transition temperatures (4). So, higher levels of DOPC provide

higher release rate from liposome because of gap between media temperature of 4°C and 37°C in comparison to DOPC transition temperature that will lead to decreasing liposomes surface stability and increasing leakage rate. Our results are in agreement with a study, which showed that using higher rigid phospholipid components with higher transition temperatures is directly related to more stable liposomes and decreased diffusion rate of active compound (5).

All three liposome formulations have shown different DL and LE capabilities, which may have influenced the release rate from liposomes. Our results showed that the highest DL and LE were obtained in the (50:50) formulation while the lowest DL and LE were obtained from the (70:30) formulation (table 2.1). These findings suggest that 50:50 formulation is optimal to achieve the best sulforhodamine B loaded liposomes because of higher encapsulation rates associated with higher DPPC content preventing loaded molecules from being leaked. The variations in DL and LE could be due to the change in the liposome membrane fluidity, which depends on differences in both the phospholipid composition and phase transition temperature.

Comparatively to liposomes, in NIPAM-co-MAA microgels using higher MAA ratios has resulted in higher DL and LE (table 2.1). This was occurred due to an increased negative charge on the surface of microgels and consequently more binding affinity of positively charged R6G. In contrast, using lower ratios of MAA has seemed to provide slower release rate of R6G but there has been no clear corelation explaining that in this study (table 2.2). Results showed that the release rate of R6G from microgels embedded in hydrogels was higher at 37°C regardless loading medium because of microgels thermo-sensitivity. However, better controlled release rate was achieved at 4°C from microgels loaded with R6G in HEPES buffer because they maintained their swelled state for longer period comparing 37°C (table 2.2).

In nanogels, results revealed that they had high DL and LE due to presence of positive charge on their surface, which enhanced negatively charged sulforhodamine B loading (table 2.1). Performing the release under varying thermal conditions had a mild influence over the release rate of sulforhodamine from nanogels embedded in hydrogels since they are not thermosensetive (figure 2.6B). The mild variation in release rate at different temperatures

could be due to the change in medium viscosity that affect sulforhodamine B solubility and mobility through the hydrogel networks.

The release kinetics from liposomes were estimated by the diffusion coefficient of the sulforhodamine B loaded within the liposomes phospholipids bilayer and embedded in hydrogel. Similarly, release profiles from microgels embedded in hydrogels were estimated by the affinity of the R6G to microgels and its diffusion from hydrogel scaffolds. Results obtained from each controlled delivery system depended either on diffusion-based release (liposomes), or affinity-based release (microgels, and nanogels) suggest that all systems have achieved extended release duration (section 2.3.7). However, the controlled release system based on hydrogel embedding liposome has shown a higher extended release duration comparing to the other two systems, which makes it the optimal system for controlled release purposes.

Developing an alternative polymerizing technique other than photopolymerization based on UV exposure might alter the release rate resulting in a better controlled release from hydrogel embedding liposomes system. We tested the 60:40 formulation release behavior before and after exposure to UV radiation. We found that there was increased sulforhodamine B leakage and release (figure 2.1B). This could be due to the thermal energy produced by the lamp and led to liposome surface permeation and consequently increased release rate. Another explanation for such behavior could result from oxidation of DOPC double bonds and changing liposome uniformity since this phospholipid is present in higher concentrations.

Changing phospholipids composition of liposomes could alter the release rate due to changes that will occur in liposomal stability (5), DL, and LE. Using different hydrogel type and varying its crosslinking rates might improve its biocompatibility, and rheological properties that could impact nanocarriers controlled release of active compounds (6, 7).

3.2. References

1. Gregoriadis G. Drug entrapment in liposomes. Federation of the European biochemical societies letters. 1973;36(3):292-6.

2. Gregoriadis G. Overview of liposomes. Journal of antimicrobial chemotherapy. 1991;28(suppl B):39-48.

3. Betageri G. Liposomal encapsulation and stability of dideoxyinosine triphosphate. Drug development and industrial pharmacy. 1993;19(5):531-9.

4. Papahadjopoulos D, Jacobson K, Nir S, Isac I. Phase transitions in phospholipid vesicles fluorescence polarization and permeability measurements concerning the effect of temperature and cholesterol. Biochimica et biophysica acta-biomembranes. 1973;311(3):330-48.

5. Anderson M, Omri A. The effect of different lipid components on the in vitro stability and release kinetics of liposome formulations. Drug delivery. 2004;11(1):33-9.

6. Mourtas S, Fotopoulou S, Duraj S, Sfika V, Tsakiroglou C, Antimisiaris SG. Liposomal drugs dispersed in hydrogels: effect of liposome, drug and gel properties on drug release kinetics. Colloids and surfaces B: biointerfaces. 2007;55(2):212-21.

7. Gao W, Vecchio D, Li J, Zhu J, Zhang Q, Fu V, et al. Hydrogel containing nanoparticle-stabilized liposomes for topical antimicrobial delivery. American chemical society nano. 2014;8(3):2900-7.

Conclusion

The research aimed to develop an improved active compound controlled delivery system by combining two active compound carriers in order to overcome limitations observed in the individual carriers such that it would lead to an enhanced controlled release delivery system. We have developed a structured hydrogel with embedded liposomes, microgels, and nanogels loaded with model active compounds that would be released in a controlled fashion by modifying thermal conditions and nanocarriers composition and concentration. We prepared and optimized three liposomes formulations using DOPC and DPPC phospholipids with different ratios loaded with sulforhodamine B. The release of sulforhodamine B from liposomes, hydrogel, and hydrogel embedding liposomes and varying thermal conditions was performed to evaluate the effects of temperature and varying phospholipids concentrations over sulforhodamine B release rate.

Results showed that liposome formulation with higher DPPC ratios provided better extended release duration comparing to formulations with higher DOPC ratios. Upon embedding these formulations separately loaded with the sulforhodamine B, within acrylamide hydrogels with fixed crosslinking rate resulted in a controlled release rate of 10 days. Using the same quantity of sulforhodamine B loaded within the hydrogel alone resulted in releasing most of the content within 48 hours only under the same thermal conditions. Embedding microgels with different ratios and nanogels separately into hydrogels loaded with same quantity of rhodamine 6G and sulforhodamine B respectively as in liposomes, resulted in faster release compared to embedded liposomes. Adjustment of hydrogel-liposomes based system via modifying phospholipids composition ratios provides the slowest release rate in comparison to microgels and nanogels. These findings suggest that diffusion-based release systems (liposomes) have higher potential than affinity-based release systems (microgels and nanogels) to achieve better controlled release. Embedding different nanocarriers within hydrogels has proven to be advantageous in providing a solution for increasing the stability of nanocarriers and hydrogels toward achieving an improved controlled release delivery system

Appendix

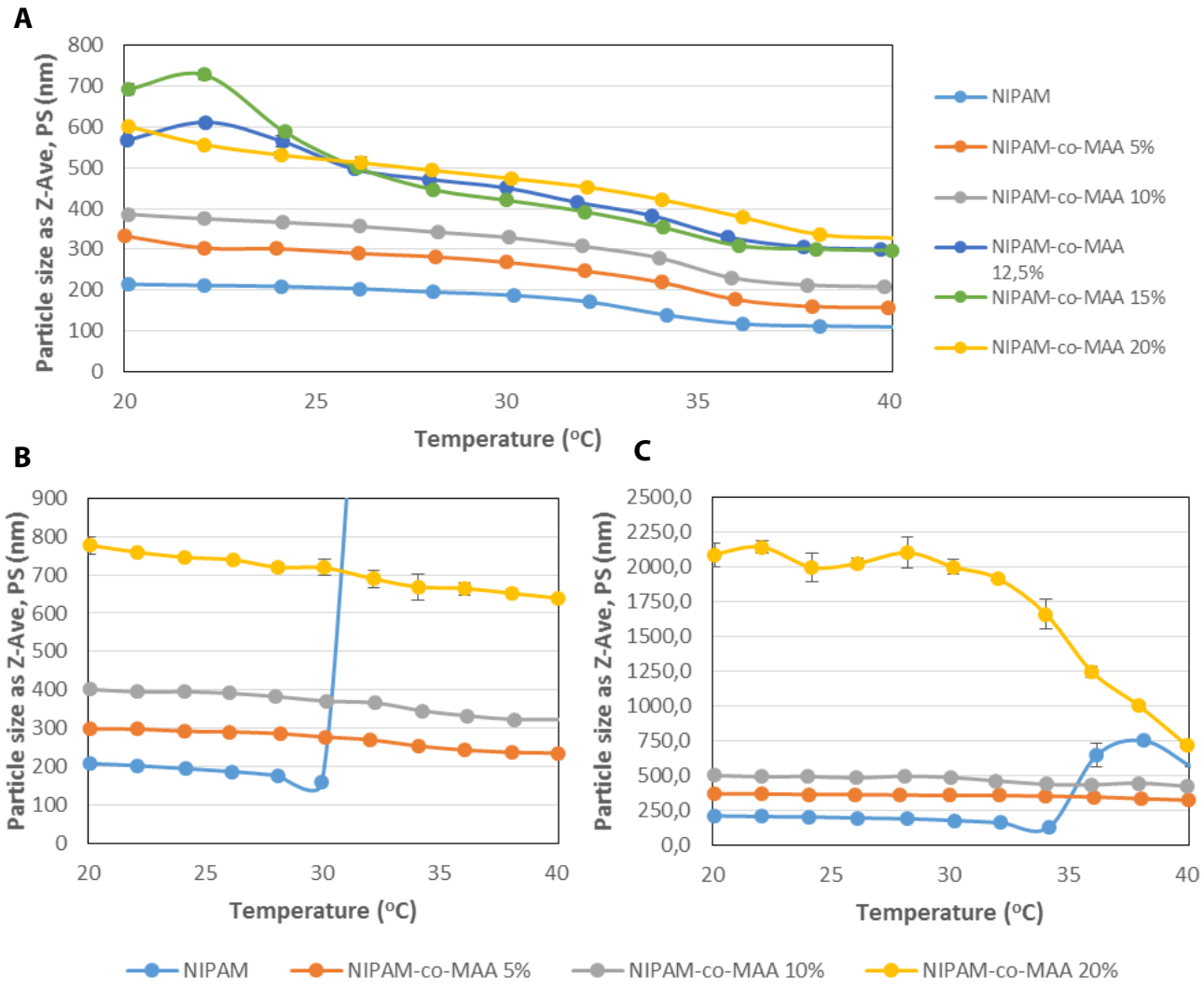

Figure S2.1. Entire microgels particle size characterizations results. Particle size, represented by Z-ave, characterization of NIPAM-co-MAA microgels in (A) pure water, (B) PBS 10 mM and 145 mM NaCl (pH=7.4) and (C) HEPES 5mM (pH = 7.4). Error bars may not be fully distinguishable for each microgels. NIPAM without MAA aggregates at 32°C resulting in high PS increases.

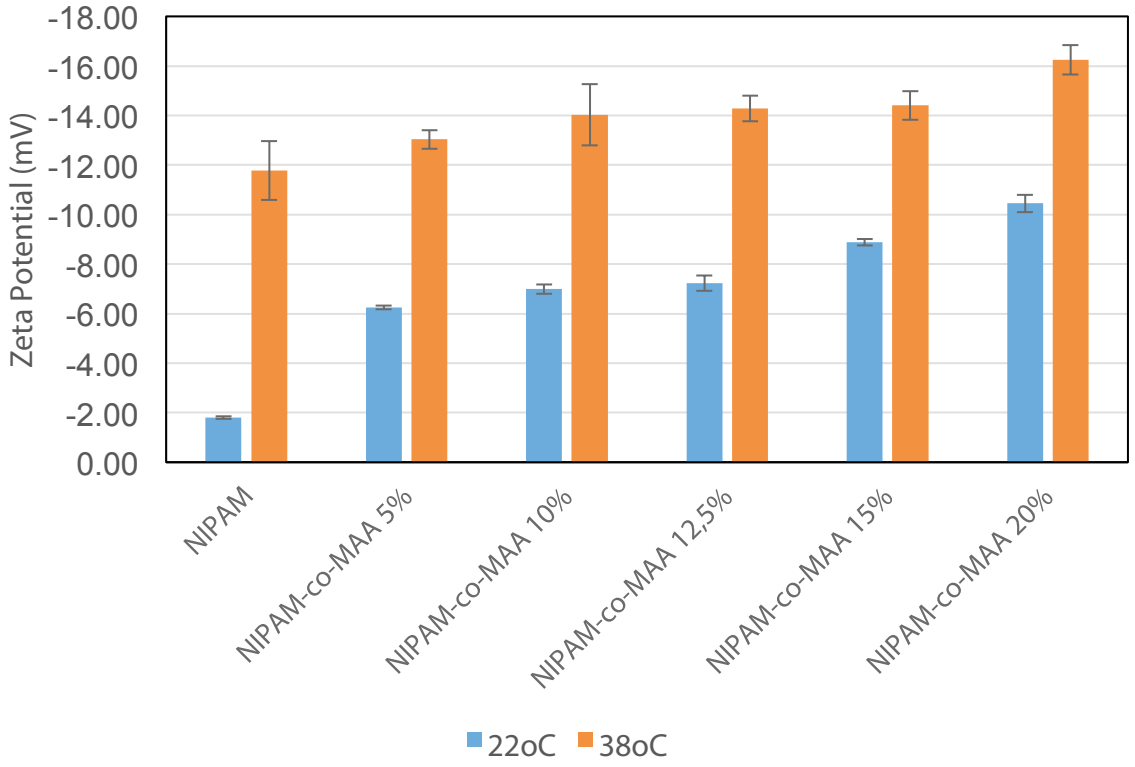

Figure S2.2. Entire microgels zeta potential characterizations results. NIPAM-co-MAA microgel zeta potential in 4 mM NaCl solution at 22°C and 38°C.